

**GROUNDWATER MODELING IN THE HIGH ANDES OF ARGENTINA:
RESOURCE ASSESSMENT AND POTENTIAL IMPACTS**

by

Juan Pablo Domínguez Rollán

A thesis submitted to the Faculty of the University of Delaware in partial fulfillment of the requirements for the degree of Master of Science in Geology

Winter 2021

© 2021 Juan Pablo Domínguez
All Rights Reserved

**GROUNDWATER MODELING IN THE HIGH ANDES OF ARGENTINA:
RESOURCE ASSESSMENT AND POTENTIAL IMPACTS**

by

Juan Pablo Domínguez Rollán

Approved: _____
Holly Michael, Ph.D.
Professor in charge of thesis on behalf of the Advisory Committee

Approved: _____
John Madsen, Ph.D.
Interim Chair of the Department of Earth Sciences

Approved: _____
Estella Atekwana, Ph.D.
Dean of the College of Earth, Ocean, and Environment

Approved: _____
Louis Rossi, Ph.D.
Vice Provost for Graduate and Professional Education and
Dean of the Graduate College

ACKNOWLEDGMENTS

I would deeply like to thank my advisor Holly Michael. Without her advice, support, and assistance this would not have been possible. Constant in-person and online meetings with her have helped me to develop my understanding of hydrology and modeling. I would also like to thank my committee members, Mike O'Neal and Neil Sturchio, for providing assistance and suggestions throughout my research.

I would not be doing this work without first have met Armando Sanchez and then Andres Meglioli from Mountain Pass LLC., for who I will be forever grateful for his support, knowledge, generosity, and wisdom. Spectacular field campaigns and work shared in the high Andes among other things have been possible thanks to him. Also, thank the unique opportunity to Minera Peregrine, Altar Mining operator for providing me with the so important data for this project, logistics, and support through the multiple campaigns.

Lastly, thank my labmates, especially Zhongyuan Xu (Tymon) for his helped and guidance in my simulations during the virtual times (pandemic) as well as my labmates who shared their advice and support. I will never forget the time spent with them both in the office and outdoors. My college friends, who made this journey enjoyable, lighter, and full of experiences. Finally, I thank my parents, siblings, and family for their unconditional support when being far from home.

TABLE OF CONTENTS

LIST OF TABLES	vi
LIST OF FIGURES	vii
ABSTRACT	xi
Chapter	
1 INTRODUCTION	1
1.1 Mountain water as a resource	1
1.2 Mountain groundwater	2
1.3 Climate change in the Andes	5
1.4 Objectives	8
1.4.1 Specific objectives	8
1.5 Research questions	9
1.6 Hypotheses	9
1.7 Background of the site	9
2 STUDY AREA	13
2.1 Location	13
2.2 Climate settings	14
3 METHODOLOGY	17
3.1 Observations	17
3.2 Data collection	20
3.2.1 Ice and water sampling	21
3.2.2 Weather parameters	21
3.2.3 Weirs	23
3.2.4 Piezometers and groundwater heads	25
3.3 Recharge rate estimates	26
3.4 Surface and subsurface domain	30
3.5 Conceptual model	32
3.5.1 Numerical model description	35
3.5.2 Numerical solution / Hydrologic model	35
3.5.3 Hydrological model setup / Model framework	36
3.5.4 Model recharge	38

3.5.5	Model parameters and calibration	38
3.6	Sensitivity analysis	43
4	RESULTS.....	46
4.1	Ice and water sampling.....	46
4.2	Weather station measurements	48
4.3	Weir data	51
4.4	Water wells	52
4.5	Snowpack distribution	58
4.6	Altar rock glacier contribution	59
4.7	Groundwater simulation results (Base case scenario)	61
4.8	Model sensitivity	66
4.8.1	Hydraulic heads	67
4.8.2	Stream discharge	68
4.8.3	Age distribution on groundwater	72
5	DISCUSSION AND OUTCOMES	74
5.1	Conclusions	74
5.2	Uncertainties in model performance	77
5.2.1	Use of a DEM and elevation differences.....	77
5.2.2	Recharge parameters and snow density estimate.	78
5.2.3	Subsurface layout	78
5.3	Future work	79
	REFERENCES	81
	Appendix	
A	SUPPLEMENTAL MATERIAL	93

LIST OF TABLES

Table 3.1:Location of weather stations	22
Table 3.2:Main characteristics of piezometers in the study area. *Piezometers within Altar watershed. (*) Water wells have been dry most of the time.....	26
Table 3.3:Parameters used for the base case scenario. (*) Values according to Fetter, C. W. (1994).....	42
Table 3.4: Plot of vertical K values versus layers. Each row represents a model layer (25 total).	45
Table 4.1:Altar rock glacier contribution estimates from 2016 to 2019.	60
Table 4.2: Backward particle tracking from P5 well and river cells. Mean travel times and standard deviation are given in years.....	73

LIST OF FIGURES

Figure 1.1: Schematic diagram showing regional-scale watersheds. (Welch and Allen, 2012).....	3
Figure 2.1: Location of the study site in San Juan Province, Argentina. The map shows the mining camp and Altar watershed.	14
Figure 2.2: Weather seasonality in the Andes	16
Figure 3.1: Instrumentation for the Altar project. Automatic weather stations (2), piezometers (8), and weirs (3). Study watershed is outlined in red.	20
Figure 3.2: Station 2, Upper watershed. (Extracted from Ingeniería y Proyectos Ltda, 2019. Weather stations maintenance.).....	23
Figure 3.3: V-notch weir at the outlet of Altar watershed. After construction (left side) and after a year (right side). (W1, Figure 3.1). Notable erosion after a year is observed on the v-notch.	25
Figure 3.4: Comparison of three different data sets (CORDEX, Pelambres, and Altar) and two parameters (rainfall and calculated snowmelt) according to hydrologic year. Left y-axis snowmelt. Right axis, rainfall. Note that snow density values calculated from the Pelambres dataset were used to calculate snowmelt using the Altar snow height values.	29
Figure 3.5: Digital elevation model of Altar watershed.	32
Figure 3.6: Conceptual model of Altar – Top view.....	34
Figure 3.7: Conceptual model. Cross section of Altar watershed.	34
Figure 3.8: Recharge rates for the transient simulation. Each month represents a stress period of a total of 84.	40
Figure 3.9: Hydraulic conductivity distribution for the base case scenario. Three main layers and two different zones (converted to one) with a higher zone than surroundings. These zones have always a K similar to the surface according to the scenarios.	42
Figure 3.10: Location of the model observation wells (red squares).	44
Figure 4.1: Tritium activity (TU) vs. time for water recharged in 1967 during period of peak tritium activity (red) and for water recharged in 1950 with pre-bomb natural tritium activity. Ice samples, as well as groundwater from the P5	

and Rio Tinto-1 monitoring wells, have tritium activities consistent with pre-bomb precipitation.	47
Figure 4.2: Weather station temperature data from January 2013 to January 2020 (gaps in the data exist).....	49
Figure 4.3. Weather station data from January 2013 to January 2020. A: Precipitation data from upper station. B: Precipitation (blue bars) and snowfall height (grey shadow) from lower station.....	50
Figure 4.4: Water depth over a v-notch weir at the outlet of Altar watershed from April 2019 to March 2020.	52
Figure 4.5: Creek water stage versus discharge for the weir at Altar watershed.	52
Figure 4.6: A: Water table vs precipitation for piezometer P1. Elevation 3705 m.a.s.l. B: Water table vs precipitation for piezometer P5 Elevation 3480.4 m.a.s.l. Time-lapse 2016-2020. Red triangles indicate data logger removal and the start of a new data long-term deployment. Gaps in data indicate lacks of measurements. Snow height data from lower weather station.	54
Figure 4.7. A: Water table and precipitation for piezometer P6. Elevation 3105 m.a.s.l. B: Water table vs precipitation for piezometer P7. Elevation 3103 m.a.s.l. Red triangle indicates data logger removal and the start of a new data long-term deployment.	57
Figure 4.8: Water table vs time for piezometer P8. Time-lapse 2018-2019. Elevation 3054 m.a.s.l. Red triangle indicates data logger removal and the start of a new data long-term deployment.	58
Figure 4.9: Snow height distribution and average temperature from 2013 to 2019.....	59
Figure 4.10: Base case scenario results. A: Heads observed and simulated for P1. Note that discrepancy is likely due to perched aquifer conditions and recharge from the rock glacier, neither of which is included in the model. B: Head observed and simulated for P5. Note that head discrepancy is likely a result of inaccurate elevation measurements and DEM data.....	64
Figure 4.11: A: Base case scenario results. Monthly stream discharge over the v-notch weir vs recharge rates and observed weir levels. B: Simulated daily heads for the transient period at Piezometer 5 at the outlet of Altar watershed. Monthly recharge rates are shown as bars.....	65

Figure 4.12: Particle tracking to well P5 and the stream. A: Plan view for well particles. B: Side view for well particles. C: Plan view for stream particles. D: Side view for stream particles.	66
Figure 4.13: Simulated heads for the transient period A: Piezometer 1, next to Altar rock glacier. B: Piezometer 5 at the outlet of Altar watershed. Recharge rates are shown as bars.	70
Figure 4.14: Stream discharge for the four scenarios.	71
Figure A.1: Precipitation from Pelambres Mining (Chile), according to the hydrologic year (April-March since 1992-2020). Source: Pelambres Mining	93
Figure A.2: Borehole data from Altar site according to elevation bands and RQD (rock quality design)	94
Figure A.3: Borehole data from Altar site according to elevation bands and RQD (rock quality design)	95
Figure A.4: Borehole data from Altar site according to elevation bands and RQD (rock quality design)	96
Figure A.5: Likely cross-section of Altar watershed according to borehole data. Columns represent the 6 elevations bands (3500-4100 m.a.s.l). Numbers within the columns show the average RQD within the layer considered on the left side and standard deviation on the right.	97
Figure A.6: A: Water table and precipitation for piezometer P5. Heads are according to DEM elevation pixel at the well (3477.08 m.a.s.l). Well casing: 0.45 m. B: Water table elevation and temperature for piezometer P5. Time-lapse 2016-2020. Alt. 3480.4 m.a.s.l.	98
Figure A.7: A: Water table elevation and temperature for P1 next to a rock glacier. Alt. 3705 m a.s.l. B: Same that above for piezometer P6. Alt. 3105 m.a.s.l. Red triangles indicate data logger removal and the start of a new data long-term deployment. Gaps in data indicate lacks of measurements.	99
Figure A.8: Water table and temperature for piezometer P7. Alt. 3103 m.a.s.l. Red triangle indicates data logger removal and the start of a new data long-term deployment.	100

Figure A.9: Hypothesized elevation profiles of the dominant components of surface ablation on debris-free glaciers of the semiarid Andes of North-Central Chile during the (a) early and (b) late ablation season. Extracted from Ayala et al., 2017..... 101

ABSTRACT

Groundwater and surface water sourced from the high Andes of Argentina are highly important for societal, agricultural, and domestic usage in the foothills and valleys, less than hundred kilometers away from the headwaters. Despite their importance, efforts to provide estimates and predictions of surface water and especially groundwater sources and sinks have been limited. During most of the year, precipitation in the high Andes falls primarily as snow, with minimal rainfall over the summer. A widespread lack of measurements and statistical analysis in the region makes it difficult to understand groundwater storage and flow patterns in the Andean watersheds. The contribution of mountain snowmelt to groundwater is a key component of recharge to this area. While this study is limited to a small watershed in the Altar valley of the Central Andes of Argentina, it is representative of most of the Dry Andes region, which runs from Bolivia south to a latitude of 35°S between Argentina and Chile. This region is characterized by steep and abrupt topography, highly fractured bedrock, and large fault systems. Here, we investigate the groundwater flow system through observations from pressure transducers and weather stations installed by a mining company exploring the area. We use this data to create a MODFLOW groundwater model of the watershed and develop then a sensitivity analysis to gain insight into the hydrologic system. We explore changes in hydraulic conductivity with depth and reduction in recharge due to uncertainties in sublimation and evaporation and potential future trends. We then analyze heads, surface outflows to assess the impact of these changes within the hydrologic system. In addition, ages distribution in particles from the one well and the river are analyzed.

This research contributes to the understanding of groundwater recharge and discharge estimates and the hydraulic behavior of upland mountainous watersheds toward better water management in the area.

Chapter 1

INTRODUCTION

1.1 Mountain water as a resource

Mountainous regions have experienced multiple and important changes over the last decades as a result of climatic change and land use modification (Briner et al., 2012; de Jong, 2015). These regions occupy 25% of the Earth's land surface, and support around 40% of the world's population who depend on rivers originating in mountain regions for their water supply (Viviroli et al., 2019). Although these regions contain important water storage systems, there is limited understanding on groundwater flow due to the scarcity of field-based studies in high-elevation watersheds and the hardships involved in conducting them (Hayashi, 2019). In mountainous environments snowpack and groundwater coupled with debris-rich landforms such as talus slopes, fans, moraines, and rock glaciers are key components of the hydrologic system either for aquifers (Hayashi, 2019) or where watercourses run all year long (Alford, 1985; Wohl, 2000; Viviroli and Weingartner, 2004; Wilson and Guan, 2004; Manning and Solomon, 2005). These mountainous waters stores are also a highly valued source of water in semiarid and arid regions where precipitation and recharge are scarce at lower elevations (Alford, 1985; Smerdon et al., 2009; Neilsen et al., 2010). Due to the effects of environmental lapse rates, mountainous areas receive more precipitation than lower altitude valleys, and the winter snow accumulation in the high terrains is gradually released towards valleys and creeks during the spring/summer snowmelt season. Therefore, surface water and especially

groundwater flow processes in mountain systems play an important role in valley water recharge either for flora and fauna, water supply for downstream communities, irrigation, or hydropower generation (crucial for arid mountainous regions).

1.2 Mountain groundwater

Despite the belief that mountain watersheds may not have a significant water storage capacity due to coarse sediments and steep slopes that allow water to move quickly through the subsurface, it has been shown that groundwater is a key component in mountain catchments (Clow et al., 2003; Hood et al., 2006; Williams et al., 2006) and a major hydrologic contributor in some parts of the Andes. For instance, Baraer et al. (2015) states that groundwater in Cordillera Blanca (Perú) contributes 24-80% of the stream discharge in four proglacial watersheds during the dry season.

Groundwater recharge and runoff in mountainous watersheds originates in mountain block recharge (MBR) (Figure 1.1), where groundwater flowing through bedrock and alluvium/colluvium is an important contribution component to basin aquifers (Wilson and Guan, 2004). In semi-arid mountainous regions, streams are able to flow year-round due to baseflow generated by deep groundwater flow through bedrock (Uchida et al., 2003; Katsuyama et al., 2005). Contribution of granite bedrock groundwater and bedrock permeability are especially important in steep slopes, which could be a key component to baseflow and groundwater (Uchida et al., 2003). While high flow periods are short with peaks during spring that depend on snowpack availability and timing of snowmelt, low flows during winter and summer seasons are steadier from season to season. Such behavior highlights that groundwater storage in mountain environments is crucial for maintaining flow without additional snowmelt or rainfall contributions (Hayashi, 2019). Groundwater flow is influenced by topography

and a combination of recharge and hydraulic conductivity characteristics (Forster and Smith, 1988; Haitjema and Mitchell-Bruker, 2005; Gleeson and Manning, 2008).

A good understanding of groundwater flow and its recharge pattern is important for sustainable water resource management (Kao et al., 2012). The use of hydrological models has been shown to be the best approach to replicate conditions that are otherwise hard to assess. Such models provide insight into complex groundwater flow systems and predictions on future behaviors (Nyende and Vermeulen, 2013).

Mountainous regions are usually characterized by a surficial layer of higher-permeability weathered and fractured rock, which overlies lower-permeability crystalline rock (Kao et al., 2012). Due to these characteristics, groundwater is directly recharged through infiltration from precipitation as either rain or snow.

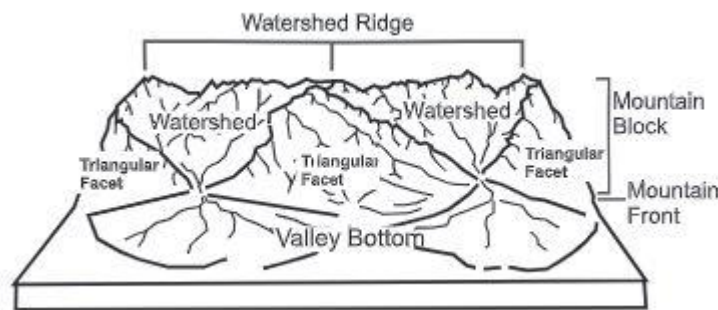


Figure 1.1: Schematic diagram showing regional-scale watersheds. (Welch and Allen, 2012).

In alpine watersheds, the hydrologic regime is fed by basin storage through groundwater and snow in high altitudes that is slowly transferred to rivers when the weather warms in spring, and to a lesser extent rainfall (Staudinger et al., 2017). In mid-latitude arid regions, between 50% and 80% of the annual water supply comes from mountainous terrain whose headwaters are snow-covered (Wahl, 1992).

The importance of the Andes hydrologic system is highlighted by Mark et al. (2005), who suggest that snow and ice from ice-fields in Peru supply up to 58% of downstream water. These two transient types of stored water have seasonal accumulation and contribution that are critical for the hydrologic system, as only 0.5% of the Andes is covered by permanent snow and ice (Mulligan et al., 2012). Due to their dependence on both precipitation and temperature, mountainous watersheds in semiarid regions are extremely sensitive to climate change (Barnett et al., 2005).

Smerdon et al. (2009) stated that groundwater recharge was found to vary from high recharge at higher elevations to lower recharge rates at lower elevations. Parameters such as precipitation, evapotranspiration, and temperature showed significant changes with elevation on a mountainous watershed with seasonal snow cover in Spain, where groundwater contribution to total outflow ranged between 70% and 97% (Jódar et al., 2017). Such results highlight the significance of groundwater recharge in high mountain areas.

Hydrologic processes such as runoff, recharge, evapotranspiration (ET), and precipitation (as rain or snow) all vary in time and space, and are related to each other, which prompts the need to analyze them in an integrated framework and model these processes simultaneously. Forster and Smith (1998) describe in detail the multiple factors that are crucial in controlling groundwater flow and heads in mountainous terrains. Predicting the water table in mountainous relief can be difficult due to uncertainties that control and influence it, such as topography, geology, climate and thermal regime (Forster and Smith, 1998).

Snow accretion and ablation are critical controls on the water budget and hydrological behavior during the melt season (Welch and Allen, 2012). Unfortunately,

data regarding these processes in mountain catchments, especially in the Andes, are lacking. This lack of measurements and statistics on common hydrological parameters due to the poor access to sites, extreme working conditions, and unpredictable weather, all of which inhibit any year-round research in this region.

The groundwater processes and interactions between groundwater and surface water in mountainous regions have been investigated (Voeckler et al., 2014; Gebreyohannes et al., 2017; Smerdon et al., 2009; Jódar et al., 2017; Welch and Allen, 2012; Welch et al., 2012) but there is little work in the Dry Andes region. Studies have been carried out in a variety of sites across South America, such as Chile (Urrutia et al., 2018; Ruelland, D., 2011; Vicuña et al., 2011), Colombia (Blessent et al., 2017), Ecuador (Guzman et al., 2016), and Perú (Somers et al., 2019; Somers et al., 2016; Baraer et al., 2015; Baraer et al., 2009). However, in the Dry Andes, especially the Argentinean Andes (Delbart et al., 2015), studies on groundwater flow and recharge are scarce and there is still a large data gap to bridge. No clear understanding exists on water budgets, groundwater and surface interactions, and their controlling variables. This research could fill a regional gap in the Andes and contribute to understanding important hydrological functions of groundwater in mountainous terrains.

1.3 Climate change in the Andes

Snow-driven watersheds are expected to be severely affected by climate changes in common decades (Mata & Campos, 2001; Kundzewicz et al., 2008). The effects of both the Southern Oscillation (ENSO) (measuring standardized differences in atmospheric pressure) and El Niño (increase in precipitation) impact precipitation in the Andes (Waylen et al., 2000). However, climate changes exacerbated by

greenhouse gas emissions (Intergovernmental Panel on Climate Change, 2001), could be potentially dangerous in mountain watersheds where any change in the already low water budget could have significant negative impact on the environment (Clow et al., 2003). In fact, higher temperature increases are anticipated to affect high mountains more than lower elevations in South American countries like Ecuador, Peru, Bolivia and northern Chile (Bradley et al. 2006, Souvignet et al., 2010). Results among models for South America are summarized by: 1-summer precipitation increase over the northern Andes and southeastern South America, 2-an overall decrease of winter precipitation, and 3-decrease of precipitation along the southern Andes for all seasons (Vera et al., 2006). More specifically, research on future scenarios for the Andes region is not encouraging because it suggests the central Andes region will likely experience a significant temperature increase of $\geq 2^{\circ}\text{C}$ over the next 80 years, which will impact the snowpack accumulation and snowmelt-runoff (Bradley et al., 2004). Such rise will impact the dry Andes faster and higher than lower elevation (Bradley et al., 2006). By the end of the century Vicuña et al. (2011) predict a warming of $3\text{--}4^{\circ}\text{C}$ and drying of $15\text{--}35\%$ of present values along the subtropical Andes. Furthermore, several studies have been conducted on the Chilean side near the study site of this research (Schaffer et al., 2019, Souvignet et al., 2010). Findings point out a longer dry season and a temperature rise which will likely impact the hydrological cycle in the area and specially the snow accumulation and melting periods. Precipitation in north-central Chile has decreased since measurements in the middle of the 19th century started (Vuille & Milana, 2007). Average precipitation in La Serena (westwards from the study site on the Pacific coast) has decreased from 170 mm in the early 20th century to less than 80 mm nowadays (Novoa & Lopez, 2001), likely due to climate

change. At the arid Upper-Elqui sub-basin, on the Chilean side as well, results from downscaling models show a negative trend on precipitation of -4.7% decade⁻¹ on average and a positive trend in temperatures ranging from 0.14 to 0.58°C decade⁻¹ in high altitudes and lower maximum temperature value at lower altitudes (Souvignet et al., 2010).

Predicted climate-driven changes could have a significant impact in the Andes. A shift in temperature would affect the hydrology of the region by decreasing annual streamflow and altering streamflow timing with a decline (increase) in streamflow over spring/summer (winter) when the demand is highest (Barnett et al., 2005; Vicuña et al., 2011). Not only would the snow accumulation process be affected, but also glacier retreat. These changes in temperature and precipitation may have a great impact on the availability of water for domestic use, agriculture, industrial activities, and hydropower (Bradley et al., 2006, Mata & Campos, 2001). Considering that many Andean countries rely on hydropower as the main source of electricity generation, water bodies can be highly affected by less stream discharge, higher evaporation rates and thus less electricity generation.

1.4 Objectives

The necessity to gain in-depth understanding of Andean watersheds and potential competition for limited water resources from future operations of mining operations in the river headwaters of the Central Argentinean Andes requires careful assessment of groundwater behavior and sustainability in terms of inflows and outflows of the basin. Mining operations require significant water resources for various processes but their impact must be minimal on the groundwater flow to limit impact on the local and down-valley environment. Toward that goal, this study aims to (1) characterize the hydrological flow system of a representative Dry Andes mountainous watershed, (2) use hydrochemical measurements to help understand the groundwater flow system, (3) incorporate a unique dataset of climatological data (precipitation and temperature) and geotechnical surveys above 3000 m a.s.l. to elucidate groundwater recharge and flow, (4) develop and assess a numerical flow model and groundwater storage in the Altar valley through MODFLOW modeling, and (5) assess the potential impacts of climate change on the watershed.

1.4.1 Specific objectives

- Develop a conceptual model of the watershed and delineate the conditions and parameters that impact the watershed.
- Develop a groundwater flow model using Model Muse within the study area.
- Use precipitation data as the recharge input of the groundwater model and compare simulated head results with piezometers installed for this project. Analyze streamflow discharge from model with weir data from site.

1.5 Research questions

1. What is the effect of hydraulic conductivity changes on the groundwater flow system?

Sensitivity to hydraulic conductivity will be assessed in model simulations.

2. What impacts do sublimation and climate change have on the hydrologic system?

Uncertainty regarding the volume of snow/ice lost to sublimation and the climate-change effects on precipitation in the Andes are assessed through a different recharge scenario in the watershed.

1.6 Hypotheses

- Groundwater age increases with increasing hydraulic conductivity values at depth.
- Stream discharge is strongly dependent on recharge from the previous season rather than from long-term average recharge.

1.7 Background of the site

The Andes mountain range is the longest mountain range in the world, and the second highest after the Himalayas. The Andes Mountains span 7200 km along the western region of South America, from the Caribbean coast to the southern extreme of the continent through 7 countries: Colombia, Venezuela, Ecuador, Bolivia, Peru, Chile and Argentina. The Andes range in width from 200 to 700 km, and reach a maximum elevation of 6961 m.a.s.l at Aconcagua Peak.

With steep terrains, strong winds, high solar radiation rates, and variable weather conditions, the Andes is a large water resource for all the countries that it crosses through. Most of the water resource is highly demanded for agriculture,

industrial, and domestic activities by cities and towns. Our research site is part of the headwaters of the main river that feeds the population of San Juan, Argentina. These aspects highlight the importance of collecting data in these mountainous watersheds, which turn is difficult due to the lack of gauges with statistical and long period records especially at high elevations where access and maintenance are difficult (Ossa-Moreno et al., 2019). Most of the high Andes remain covered by snow and glacier bodies above 5500 m.a.s.l. over a rocky terrain where vegetation is sparse and mostly present along springs and creeks.

At the Altar study site (Figure 2.1), research has been carried out to delineate aquifers. Vector Argentina (2008) stated that aquifers are more likely to be found in the Quaternary sedimentary filling, mainly in the alluvial plains that show a well-developed thickness. They performed vertical electrical sounding (VES) in order to explore the subsurface along La Pantanosa river alluvial plain, which has an extension predominantly west-east. VES results showed the emplacement of two layers: (1) an upper layer of up to 15-20 m thickness filled the former glacier valleys and (2) a lower layer, corresponding to bedrock, developed likely secondary porosity in its upper section. Also, Teotop (2011) carried out a similar VES survey but covering a bigger area along the same river, reaching all the way to the headwaters of Quebrada de Mina valley (QDM). The same two hydrological layers were identified. The lower layer was correlated with intrusive and volcanic rocks (granites, andesites, and rhyolites) from the Choiyoi Group. These rocks were shown to be fractured and may have aquifer properties with secondary porosity and permeability. The upper layer showed thick sediment deposits correlated to glacial deposits, which form the most important aquifers, and secondly fluvial sediments which both fill valleys and ravines. In some

cases, drillings in the valley area showed a glacial till thickness of 167 m (Alfarcillo valley, next to Altar valley) and 224 m (P7 well, Figure 3.1) highlighting the significant thickness of the upper glacial layer in these locations. It is also important to consider the role of hillside sediments (colluvium) which have high porosity and permeability and therefore are a pathway for water infiltration from snow melt or rainfall. Because these permeable sediments are located on steep slopes, water does not accumulate and infiltrates rapidly. Studies carried out by Ansilta (2010) applying a geophysical survey have identified the same characteristics.

Teotop (2011) estimated the water reserve in the area based on geoelectrical prospecting and drillings. It was determined that the area with the greatest thickness of sediments carrying groundwater extends along La Pantanosa river valley (west-east direction), about 2 km upstream and downstream of the Altar Camp, and has a potential volume of storage water $\sim 3.8 \times 10^7 \text{ m}^3$. The estimated volume is approximately the same as the potential water demand for mining for a 3-year period.

Mountain Pass (2015) has carried out annual surveys since 2010 that include glacial and peri-glacial landforms monitoring and contributions to the hydrological balance of the area, and temperature monitoring that helps to constrain permafrost distribution in Altar project area. Permafrost model results do not fully agree with the observed presence in the terrain, thus it remains a challenge to estimate the contribution of permafrost to the hydrological system. In this context, it is thought that the permafrost is likely dry, which would imply minimal impact on the hydrologic balance. Permafrost thickness can be highly variable in the area and influenced by elevation, radiation, exposure, and relief. A geochemical study of water solutes and stable isotopes conducted by Burkhart (2014) states that data on stream flow did not

show evidence of substantial contribution of melt water from rock glaciers. Most of discharge in the area is apparently influenced by snowmelt, indicating that the seasonal snow pack is crucial for sustaining discharge from these watersheds.

The Quaternary geology of the field site is composed of a variably thick layer of glacial deposits that were likely moraine deposits subsequently modified by fluvial processes. Groundwater recharge and flow occur within and over these layers. The topographic relief shows also alluvial fans, alluvial plains, and landslides on site. Below the Quaternary sediments, a Cretaceous marine sediment formation overlies a Permo-Triassic granite and andesitic volcanoclastic rock, which belong to Choiyoi Group and are highly weathered (Vector Argentina, 2008).

Chapter 2

STUDY AREA

2.1 Location

The study area is located along the Andes Main Cordillera of Argentina, in the center-west of the country within San Juan Province (Figure 2.1). The area is part of the headwaters of San Juan River, the main river of the region. This large watershed spans an area of around 25,500 km² and has an annual river discharge of 2×10^9 m³/yr (Teotop, 2011).

Altar and its surroundings are a typical Andean watershed presenting steep slopes, big boulders and outcrops, rocky terrain, and some irregular grasslands along the creek, which eventually become wide and green valleys called vegas. The remote location of the site, its high altitude, and extreme winter weather limit access to the site except during the summer period from January to April. The project site is located at an elevation of approximately 3100 m.a.s.l. and corresponds to a mining property named Altar. On the site there is a mining camp which is the base for all the operations carried out on the two main valleys and mining targets, QDM and Altar.

The study area is located north of the Altar camp and is centered at latitude 31°32'18" S and longitude 70°28'08" W (Figure 2.1). The Altar watershed is delimited at the north, east and west boundaries by mountain ridges that enclose Central and East Altar, respectively, and southward by a small non-permanent creek that discharges the surface water outflow from the valley. The watershed covers an area of 5 km² and spans an elevation range from 3500 to 4080 m.a.s.l.

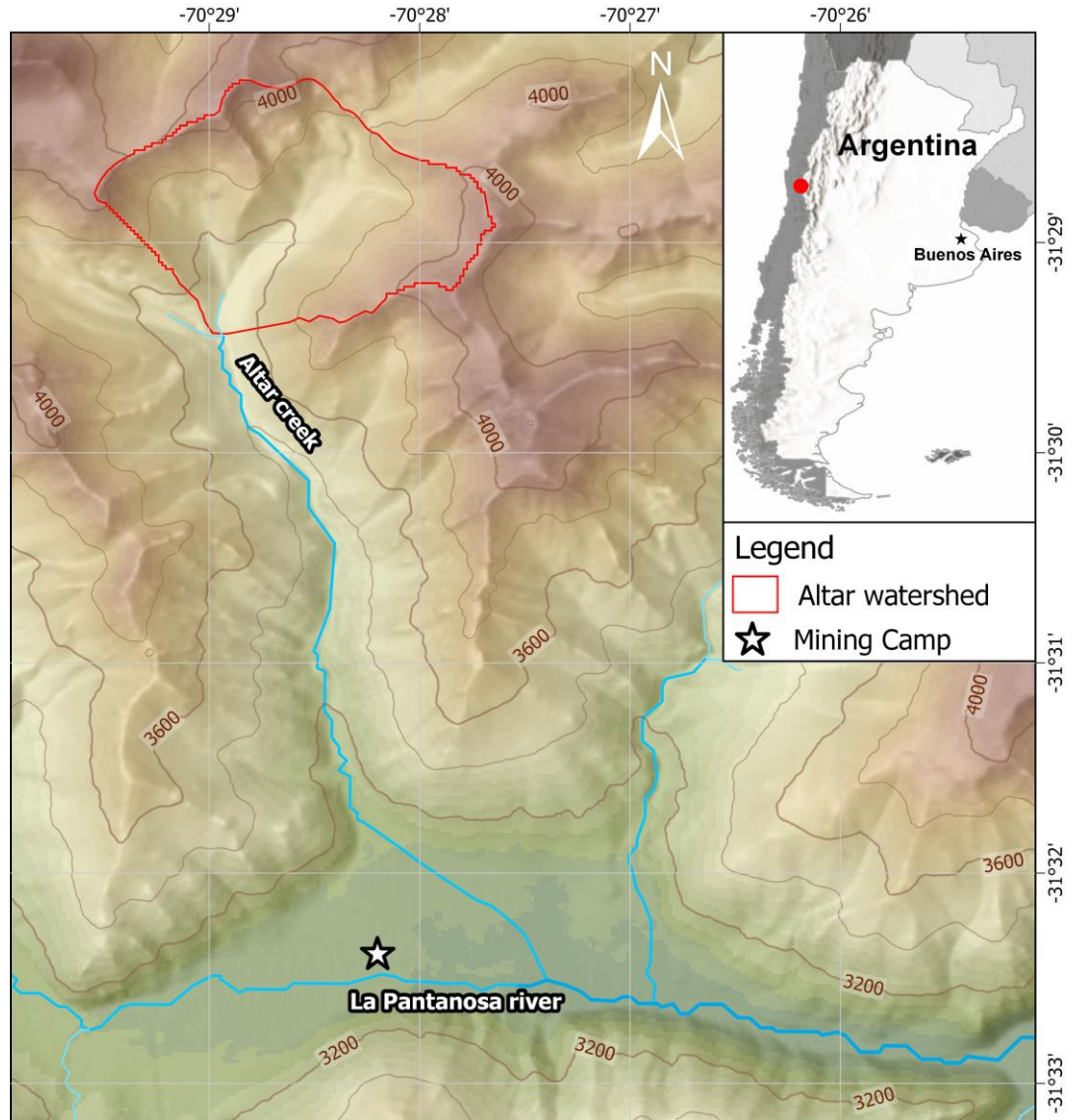


Figure 2.1: Location of the study site in San Juan Province, Argentina. The map shows the mining camp and Altar watershed.

2.2 Climate settings

Mountain ranges play an important role in configuring the climate of regions. The Dry Andes are characterized by semi-arid climate with marked seasonality (Figure 2.2). The summer is mostly dry with scarce rain, and most of the precipitation

falls mainly as snow during the months of June, July and August. Annual average precipitation ranges from 280-300 mm and is highly influenced by orographic effects causing more precipitation on the windward side (Chile) than the leeward side (Argentina) of the Andes (Viale and Garreaud, 2015; Viale and Nuñez, 2011). Moreover, high solar radiation throughout the year (Schrott, 1998) and high evaporation rates, in some cases up to 1200-2400 mm per year, which greatly exceed the annual precipitation (Albrecht, 2012) are factors that influence the area. A reduction in precipitation occurs from west to east as the elevations diminish. Whereas precipitation in this part of the Andes can reach 300 mm (snowfall and rainfall) it drops to an average of 135 mm in Barreal valley at the foothills of the Andes (31°38'S, 69°28'W, 1644m a.s.l.) or 100 mm in San Juan, the main oasis in the province (31°32'S, 68°31'W, 635m a.s.l.). Temperature patterns are seasonal, with melting processes in spring and monthly air temperatures >0°C from ~November to April, whereas sub-freezing temperatures occur in May throughout October.

The climate of the Andes Cordillera is strongly influenced by the ENSO (El Niño Southern Oscillation) phenomenon. Precipitation tends to be higher (lower) with El Niño (La Niña) showing a warm phase and a periodicity ranging from 2 to 7 yr (Garreaud et al., 2008). Annual precipitation means of ENSO range from 60-70 mm during the La Nina phase and annual maximums of 1100-1200 mm during the El Nino phase (Montecinos and Aceituno, 2003). The passage of extratropical cold fronts during the austral winters contributes more than 80% of annual precipitation between May and August (Falvey and Garreaud, 2007). In addition, the occurrence of either liquid or solid depends on the zero-isotherm location which in winter is above 3000 m.a.s.l. accumulating snow in the upper portions of the basins (Ossa-Moreno et al.,

2019) and leading to snowmelt-dominated basins. Therefore, the hydrograph is dominated by the seasonal snowpack thickness, and to a lesser extent by summer melt contribution from permafrost and glaciers.

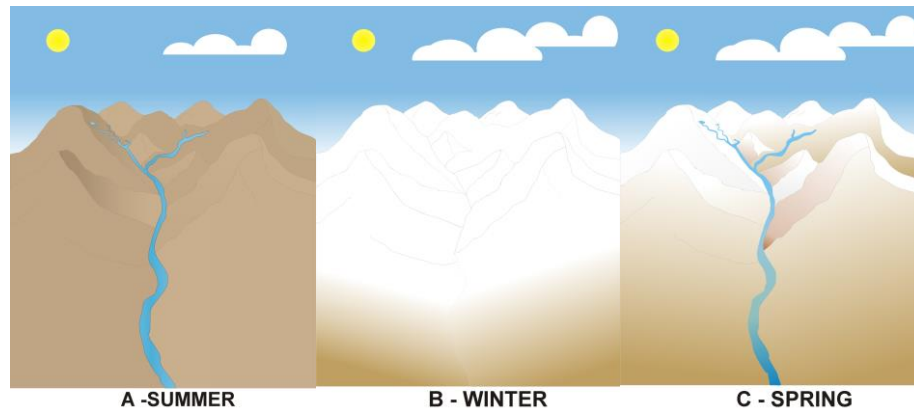


Figure 2.2: Weather seasonality in the Andes

Chapter 3

METHODOLOGY

3.1 Observations

This study characterizes groundwater flow in the region using both field data and modeling methods.

Since 2017, annual field campaigns have been carried out during the austral summer, when the mining area is accessible. These campaigns collect data from instruments installed in water wells that observed year-round measurements of water table elevation and groundwater temperature to evaluate seasonal changes in groundwater levels. The data are measured by HOBO pressure transducers in piezometers located throughout the valley near the mining camp. Such devices are able to provide an easy and accurate way to monitor and record water levels continuously for long time periods. A pressure transducer records the combined atmospheric pressure and pressure exerted by the overlying water column. Atmospheric pressure measurements were recorded by a barometric pressure transducer located in Altar valley. The pressure transducer data were corrected using records of atmospheric pressure to obtain water depth above the pressure sensor. Well elevation and depth-to-water data were used to determine water table elevation. Over the field site a total of eight pressure transducers (Figure 3.1) were set in water wells at different sites. Unfortunately, after the deployment three wells went dry (P2, P3, P4, figure 3.1). They were installed at locations from the upper Altar Valley catchment (3705 m.a.s.l.) along Altar Creek as far as the La Pantanosa River, the main surface water path of the area. Two sensors were located next to the river. This water level monitoring array covered a distance of ~8 km. To obtain the data from year to year,

annual campaigns were carried out to download data from pressure transducers in piezometers. Then, the data were processed and corrected to obtain accurate water table elevations.

Samples of stream water and glacial ice were taken during the 2018 campaign to measure hydrogen and oxygen stable isotope ratios along with solute concentrations to address the origin of the water. These analyses were performed at the UD Environmental Isotope Geochemistry Laboratory under the supervision of Dr. Neil Sturchio at the University of Delaware. Tritium analyses were performed by the University of Miami Tritium Laboratory on samples of ice from the QDM rock glacier next to Altar valley and in two groundwater samples, including one from monitoring well P5 and one from Rio Tinto 1 well (next to Altar valley and near the mining camp), to address subsurface residence times. SF₆ concentrations were measured by the U.S. Geological Survey (USGS) Reston Groundwater Dating Laboratory in water samples from these two wells.

Meteorological data was obtained from the site. Two weather stations are located in the study area, at the top and bottom of Altar valley, separated by approximately 8 km. Measurements were taken daily and monthly on variables including temperature, relative humidity, wind speed, solar radiation, and precipitation. In addition, the lower station is also able to measure snow height from an infrared sensor year-round.

Streamflow measurements have been recorded since summer 2019 following the installation of three weirs across Altar Creek. Technical, geological data, and core logging descriptions from boreholes were provided by the mining company. Geological and geophysical survey data gave insight into the subsurface and depth of

overburden and bedrock. Together these data have been used as input parameters into a three-dimensional finite-difference groundwater flow model, ModelMuse (Winston, 2009), a Graphical User Interface (GUI) for MODFLOW (Harbaugh et al., 2000) to simulate groundwater flow. This GUI was selected due to its applicability to different scenarios, ease of input file creation, relatively friendly interface, and free access on the USGS website.

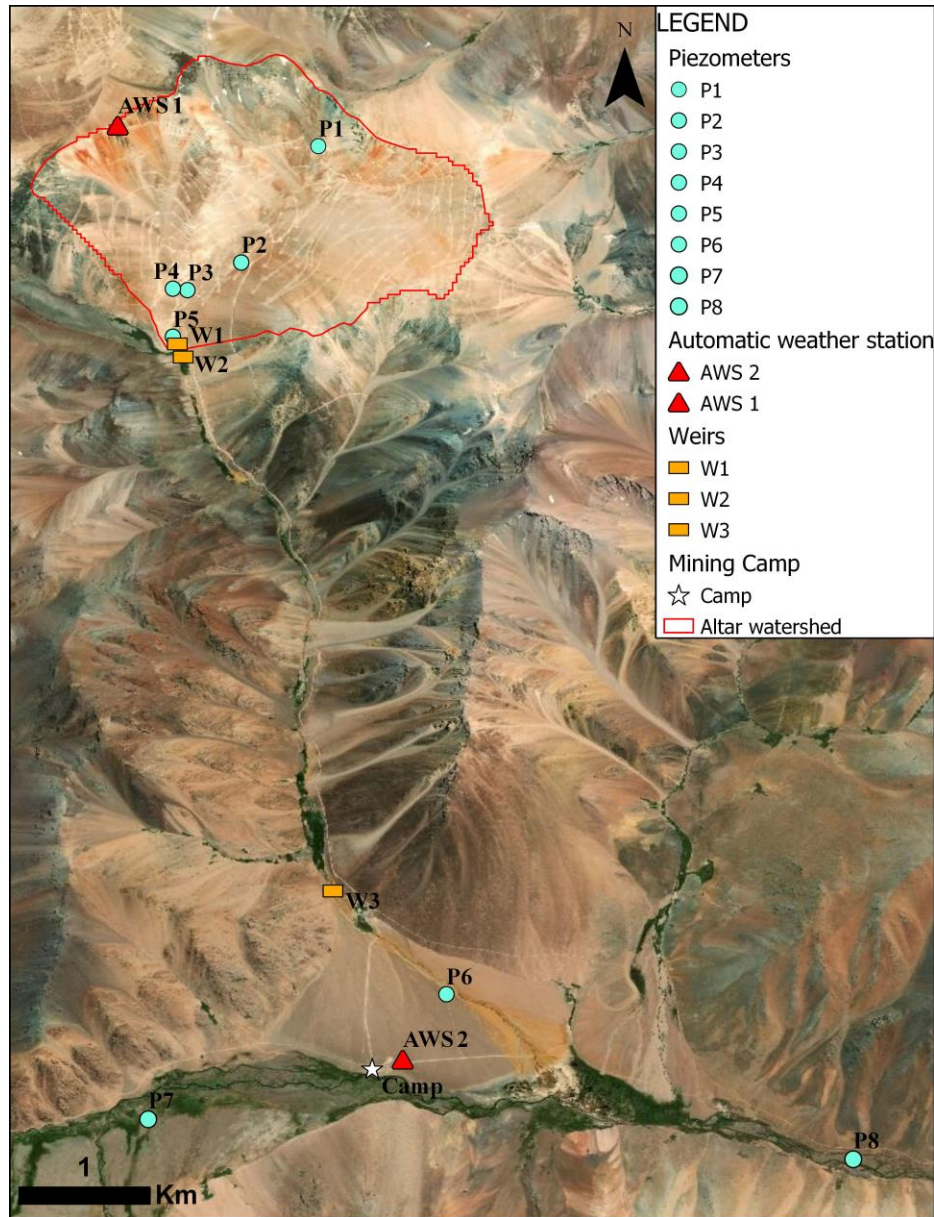


Figure 3.1: Instrumentation for the Altar project. Automatic weather stations (2), piezometers (8), and weirs (3). Study watershed is outlined in red.

3.2 Data collection

Elevation information was obtained from a digital elevation model (DEM) made available through the U.S.G.S. This DEM was used to account for the terrain

relief with 30 m spatial resolution and was masked with the boundary of the study area.

3.2.1 Ice and water sampling

Ice and water samples were analyzed for tritium, sulfur hexafluoride, sulfate, chloride, and stable isotopes of H and O. Tritium was released to the atmosphere by above-ground nuclear bomb tests during the decade of the 1950's and early 1960's and its concentration may be used to constrain the subsurface residence time of groundwater. Sulfur hexafluoride (SF_6) is a stable gas detectable in groundwater, which can be used to constrain the time of recharge of a given groundwater from about 1970 to the present (Phillips et al., 2020; USGS, 2020). Concentrations of SF_6 in natural water can be influenced by rock type, geologic history and age, aquifer characteristics, and elevation of recharge area.

3.2.2 Weather parameters

Two automatic weather stations provide weather parameter measurements for the study site since 2011 (Figure 3.1). Data are collected either daily, hourly or by the minute from both sites. Sensors measure precipitation, air temperature, relative humidity, wind speed, wind direction, barometric pressure, solar radiation, and snow depth (only measured in the lower station). The sensors are installed on a 5 m high aluminum mast and secured with wires. The data are recorded by the stations and is downloaded every summer when the mining work resumes. The locations of the weather stations are shown in Figure 3.1 and summarized in Table 3.1.

	Station 1	Station 2
Location	La Pantanosa valley (next to mining camp)	Altar upper watershed
Elevation of station (m.a.s.l.)	3088	3990
Latitude and longitude	-31°32'22.01'' S -70°28'0.87'' W	-31°28'30.88'' S -70°29'11.49'' W

Table 3.1: Location of weather stations

Rainfall was measured using a tipping bucket rain gauge at both meteorological stations. Temperature and humidity were measured through a sensor designed to support extreme weather conditions. Another crucial parameter in the area is snow depth, which was only measured at the lower station. This spot is equipped with a Judd sensor that accounts for the time required for an ultrasonic pulse to travel to and from the surface of the snowpack. The instrument has a typical accuracy of $\pm 0.01\text{m}$. To remove noise from the snow depth data sets in locations where no snowfall occurs, we used moving average filters of 4 days. This method allows smoothing of results where snow events do not occur. Increases in snow depth greater than 3 – 4 cm that lead to growth in the snowpack thickness during the winter season are not modified and thus plotted on an hourly basis. Snowmelt is the main source for groundwater recharge.



Figure 3.2: Station 2, Upper watershed. (Extracted from Ingeniería y Proyectos Ltda, 2019. Weather stations maintenance.)

3.2.3 Weirs

Runoff was measured on the study site with a 60° v-notch weir located at the mouth of the watershed and few meters downhill from the piezometer P5 (Figure 3.1). The stream gage was built in summer 2019 but has been eroded and partially destroyed due to the water acidity in the area. The weir is 0.12 m wide, 0.90 m long, and 0.50 m high. Two more weirs were installed along Altar Creek with a rectangular design that performs better for creeks with greater discharge. These two weirs have survived in better condition.

Weirs are widely used to measure discharge in flumes and open channels. They are reliable flow measuring instruments. A triangular v-notch weir was built at the outlet of Altar watershed, a few meters below water well P5 to monitor streamflow (Figure 3.3). The mining company built three weirs (one v-notch and two rectangular weirs) along Altar creek during summer 2019. The weir of interest has a triangular v-notch shape, this design was chosen since it provides greater accuracy at low flows and for small streams (Shen, 1981). It is 0.70 m x 0.50 x 0.12 m and has a v-notch angle of 60°. The materials used to build all three weirs were bricks and cement. The streambed, inner walls, and the weir sections were covered with cement in order to minimize water leakage. All three weirs were equipped with a data logger sensor that took pressure measurements every 15 min.

The recorded water levels were referenced to the bottom of the v-notch. The sensor was located in a perforated PVC pipe and deployed on the v-notch wall.

The flow equation for triangular v-notch weir is as follows (Henderson, 1966):

$$Q = \frac{8}{15} \times C_d \times \sqrt{2g} \times \tan\left(\frac{\theta}{2}\right) \times h^{5/2}$$

where Q is the volume rate of flow or discharge (m³/s); C_d is the nondimensional discharge coefficient; g is the acceleration due to gravity (9.81 m/s²); θ is the notch angle (degrees); and h is the head over the weir (m). This equation was used to compute discharge flows on the weir.



Figure 3.3: V-notch weir at the outlet of Altar watershed. After construction (left side) and after a year (right side). (W1, Figure 3.1). Notable erosion after a year is observed on the v-notch.

3.2.4 Piezometers and groundwater heads

Groundwater elevation data in the Andes is scarce, as the location is remote and installation costs of water wells are large. In order to mitigate these problems, the mining company has installed piezometers equipped with water level loggers. Water level loggers or pressure transducers can record quality data constantly without human intervention providing a deep and crucial insight into the behavior of the water resource in this region of the Andes. Seven piezometers with pressure transducers (Onset Hobo Data Loggers) were installed across the watershed from the Altar valley to the La Pantanosa River. Such devices are held by a steel cable at different depths and are constantly measuring groundwater levels and water temperature every 30 minutes. Piezometers are made of metal pipe partly screened at the bottom. Atmospheric pressure was measured by a barometric sensor located on the surface next to P5 (Figure 3.1). Data from the unvented pressure sensors were subsequently corrected to determine the phreatic surface ('water table'). Figure 3.1 shows their distribution and Table 3.2 displays their main characteristics.

PIEZOMETER LOCATIONS

ID	Latitude (S)	Longitude (W)	Ground elevation (m.a.s.l.)	Well depth (m)
P1*	-31°28'36.48''	70°28'21.80''	3705	19.50
P2*(*)	-31°29'4.60''	-70°28'40.92''	3578	80
P3*(*)	-31°29'11.7''	-70°28'54.24''	3508	39
P4*(*)	-31°29'11.29''	-70°28'57.92''	3537	53
P5*	-31°29'22.88''	70°28'57.88''	3489	15
P6	-31°32'5.71''	-70°27'50.18''	3105	138
P7	-31°32'36.72''	-70°29'3.96''	3103	224
P8	-31°32'46.98''	-70°26'9.08''	3054	80
P1' (NEAR P1) *	-31°28'36.48''	-70°28'22.07''	3695	21

Table 3.2: Main characteristics of piezometers in the study area. *Piezometers within Altar watershed. (*) Water wells have been dry most of the time.

3.3 Recharge rate estimates

Although both weather stations are almost equally equipped, solely the lower station next to the mining camp records snow height values. In addition to not having an infrared snow sensor, the upper station is positioned on a northern hillside, a leeward location and in an opposite direction of Altar watershed. These conditions may not be representative of the entire watershed. Thus, we considered rainfall and snow height values from the lower weather station due to two reasons. First, the lower location brings slightly higher temperatures and an area less prone to strong winds located in a wide valley that help the pluviometer to capture better intensity and

duration of all rainfall events, as observed in Figure 4.3B. Second, the unique presence of the snow sensor on the lower weather station is critical to estimating recharge.

Snow height measured hourly at the lower station next to camp was averaged into daily values and analyzed for each winter season. The sum of daily negative changes for each seasonal snow curve was considered as the hypothetical snowmelt for each season. This method of estimation assumes that sublimation and evaporation as well as changes in snow density are negligible (any loss of snow height from day to day is due to melt).

The short weather data history and the lack of direct snowmelt measurements led us to compare the data set with two other datasets, CORDEX and Pelambres. CORDEX is a regional reanalysis of climate data from the Coordinated Regional Downscaling Experiment (CORDEX) for the South American domain carried out by Brian Hanson and Michael O'Neal, professors at the University of Delaware (unpublished work). These data were not used directly in the recharge estimate due to the lack of a complete time overlap between CORDEX data and measurements (1980-2010 for CORDEX compared to 2012 onward for measurements) (Figure 3.4) and the low spatial resolution of the CORDEX data (approx. 165 km latitude and 145 km longitude). However, the CORDEX dataset provides a full set of valuable climate parameters, which are generally unknown at these latitudes and extremely hard to obtain in alpine and remote locations. It is also a benchmark against which we can compare our direct measurements to identify any major inaccuracies.

The second dataset includes direct measurements collected at Pelambres, a mining site located on the Chilean side 20 kilometers to the southwest of the Altar site.

The dataset is from 1992 onward and provides rainfall and snowmelt (Figure 3.4 and A.1).

Since Altar snow height measurements needed to be converted into snowmelt, we used the Pelambres snowmelt record to get an average snowmelt value. The first step involved averaging the ten annual snowmelt values from Pelambres (1994-2014). The timespan only grouped the ten years prior to when the Altar measurement started (i.e. before 2014). Once the Pelambres average snowmelt was obtained, we divided it by the Altar average snow depth differences to obtain an estimated snow density. The snow density estimated was then used with Altar snow height differences to obtain snowmelt at Altar for the period 2013-2019, since both data overlap. We assumed that the computed snow density (250 kg/m^3) remained fixed every season when computing Altar snowmelt. Despite the fact this is not the reality, our estimated snowmelt rates showed a good agreement with the Pelambres data. The mentioned snow density value is reasonable when considering that it fits within the category of settled snow according to Paterson (1994). The decision on using the Pelambres data set was based on two characteristics. First, the Pelambres rainfall data compares quite well with the Altar site, indicating that the weather is similar at the two sites. Second, the proximity of Pelambres to Altar ($< 20 \text{ km}$) was thought to be more accurate and point-based than the comparison with the CORDEX data.

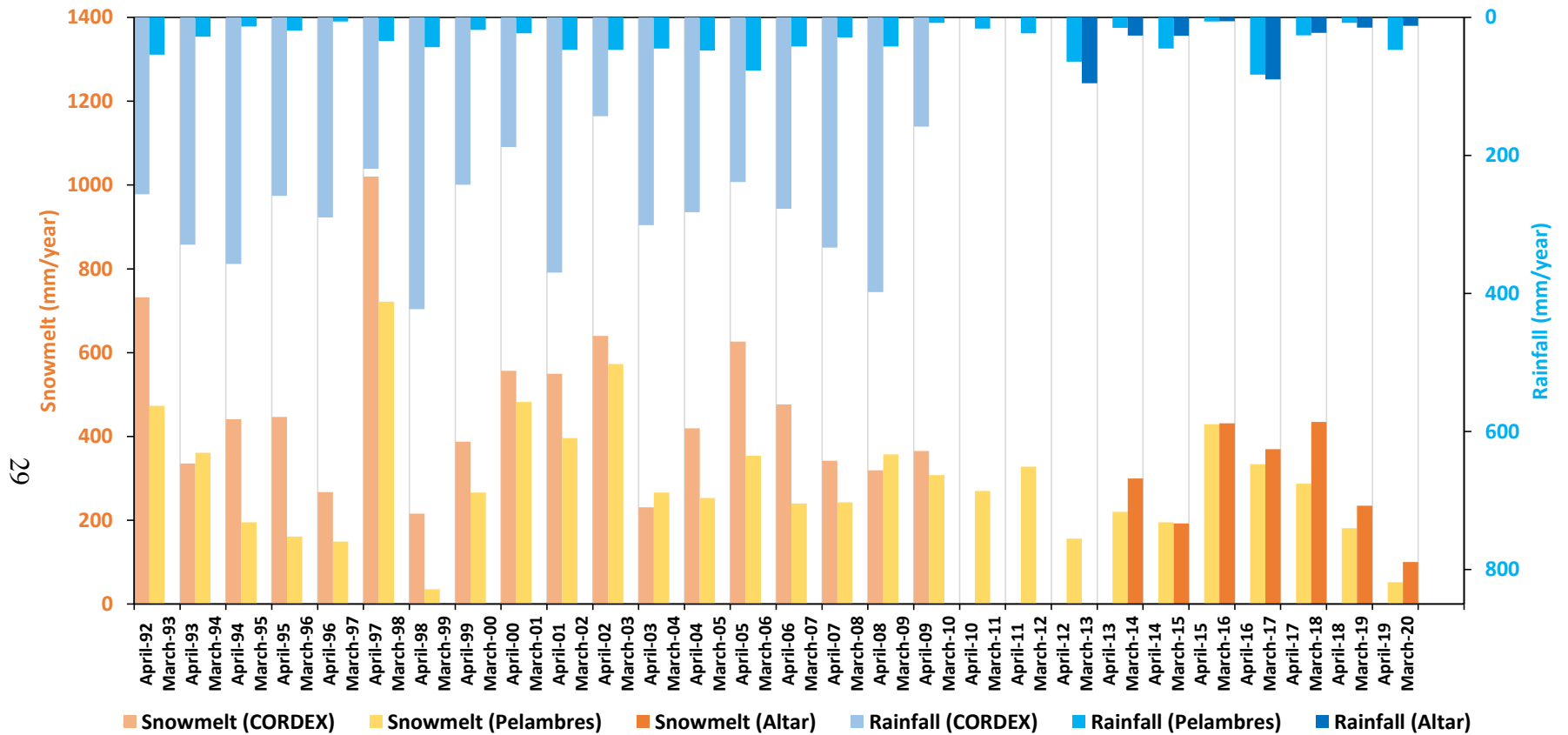


Figure 3.4: Comparison of three different data sets (CORDEX, Pelambres, and Altar) and two parameters (rainfall and calculated snowmelt) according to hydrologic year. Left y-axis snowmelt. Right axis, rainfall. Note that snow density values calculated from the Pelambres dataset were used to calculate snowmelt using the Altar snow height values.

3.4 Surface and subsurface domain

Topography was obtained through a DEM (Earth Explorer, 2000), and then imported into Model Muse. To avoid large changes in pixel elevations, the DEM was smoothed with the kriging tool in ArcGIS. This spatial interpolation method has shown to work well with raster and terrains with steep elevations. The digital elevation model was used then to configure the other layers according to borehole data and geophysical surveys (Figure 3.5).

In order to get insight into the subsurface layout, Rock Quality Designation (RQD) estimates within borehole data were provided by the mining company and analyzed. This parameter is a measure of the rock quality from the core taken from the borehole. It accounts for the number of fractures or joints in percentage, where values lower than 50% represent a fractured and weathered rock (i.e. higher K) whereas values towards 100% indicate good quality hard rocks (i.e. low K) (Appendix, Figure A.2-A.4).

A total record of 159 boreholes covered the elevations from 3500 m.a.s.l up to 4100 m.a.s.l. within the Altar watershed. The large size of Altar borehole dataset demanded processing and partitioning the dataset into a series of elevation bands. First, boreholes were classified into 100 m vertical elevation bands according to surface elevation. Secondly, the RQD percentage which was obtained every three meters through borehole analysis was averaged in 20 m vertical intervals for each borehole. Results from this process are shown in Appendix in Figures A.2-A.4. A total of six vertical bands were obtained which contained RQD percentages from boreholes within the corresponding band. Later, results from each elevation band were merged into a cross section profile in order to assess trends. Decisions about subsurface

hydraulic conductivities were based on RQD approximation values vertically within bands and laterally (horizontally) to assess layer extension (Figure 5.5).

We estimated that K varied inversely with RQD. Three main layers were identified as: alluvial fill, fractured bedrock, and basement or bedrock.

Geologic layer 1 represents the alluvium and top of the model that is aligned with the DEM which displays the topography of the watershed. This layer extends from land surface to a depth of 60 m representing gravel and rocky soil. Layer 2 represents the fractured bedrock formation and it covers the area below the alluvium (~60m) with variable depth between 180 and 340 m deep. Within this layer, the borehole data showed two small layers with lower RQD values than the surroundings. They extended solely below 3800 m.a.s.l and 3700 m.a.s.l. As a result, these two small layers were setup with higher K values than the basement. The deepest layer corresponds to basement rocks which extend between 300 and 400 m deep. We cut off the model at this depth because little groundwater flow is assumed to occur in deeper bedrock. Although on site there are bedrock outcrops on the hillsides, these have not been specified in the model and alluvium is assumed to exist all across the model top.

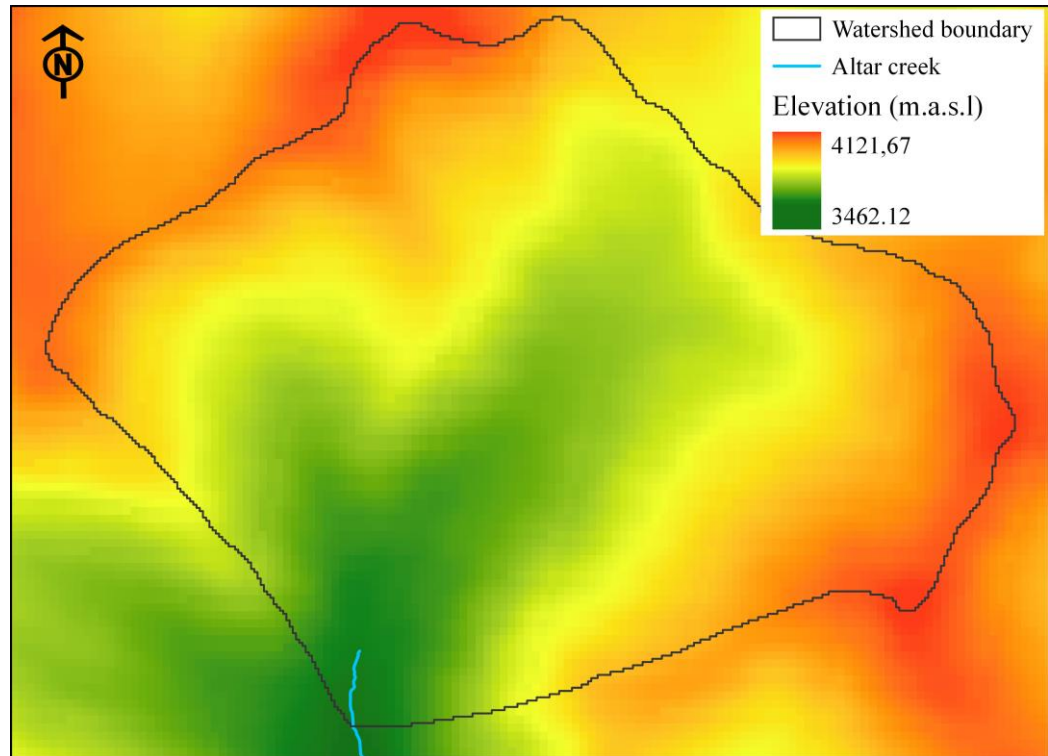


Figure 3.5: Digital elevation model of Altar watershed.

3.5 Conceptual model

A conceptual model is a simplified representation of the groundwater system which shows processes influencing the area, water inputs and outputs, boundaries and stratigraphic units. An approach of the conceptual model for Altar watershed is displayed in Figures 3.6 and 3.7. The subsurface and groundwater system is defined by three layers. The first layer represents the alluvium in an unconfined aquifer with a variable thickness across the watershed up to 60 m. Underneath the alluvium is a second layer of fractured rock that is defined and conceptualized as an unconfined aquifer. Layer 3 is part of the basement and a transition to bedrock encompassing the entire system.

The boundaries in all directions of the conceptual model are considered to be no-flow boundaries. Recharge of the aquifer occurs through precipitation either as snowmelt or rain. Discharge is assumed to occur solely through a small creek that drains the watershed on the southern boundary. Although interbasin groundwater flow is not analyzed in the present simulations, our results would suggest that this likely does occur. Connected underflow beneath mountainous ridges could be an important component of the groundwater budget.

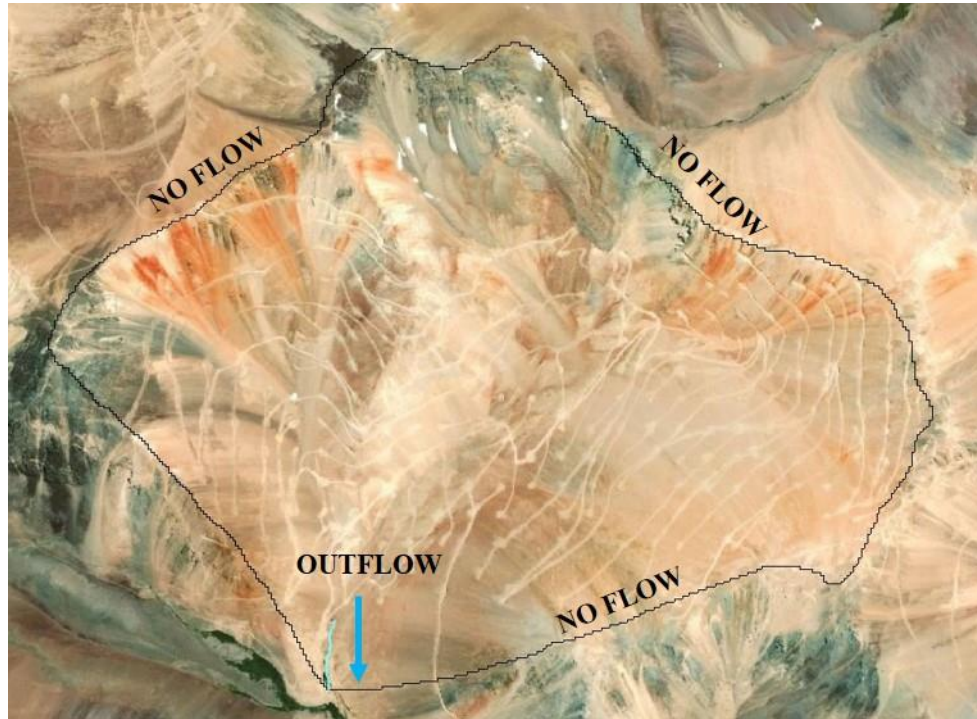


Figure 3.6: Conceptual model of Altar – Top view.

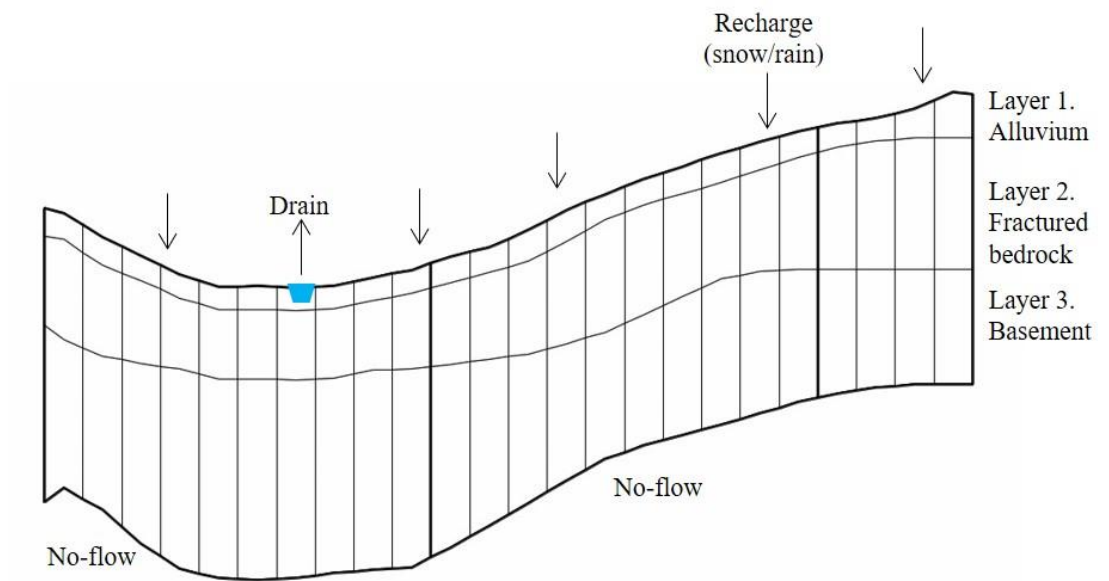


Figure 3.7: Conceptual model. Cross section of Altar watershed.

3.5.1 Numerical model description

Movement of water through an aquifer can be computed by analytical or numerical approaches. However, the analytical solution is difficult to execute due to the complexity of hydrologic boundaries, heterogeneity, and anisotropy of aquifer materials that limits its application to simple systems (Kernodle et al, 1995). Numerical models, however, are the best approaches to solve the groundwater flow equation through modeling software that allow steady-state and transient groundwater flow in three dimensions within heterogeneous media with complex boundaries (Knoti, 2018). Although, simplifications and assumptions are made when modeling, it is by far the best tool to understand aquifer systems and groundwater and surface water interaction in hydrogeologic systems with the potential to assess future scenarios and predictions under changeable conditions (Bredehoeft 2005; Vandenbohede et al. 2011).

3.5.2 Numerical solution / Hydrologic model

Groundwater flow in the area is simulated using the three-dimensional groundwater saturated flow equation of MODFLOW (McDonald and Harbaugh, 1998). Hydraulic heads in the equation are expressed through the Darcy's law:

$$q_x = -K_x \cdot \frac{\delta h}{\delta x}; q_y = -K_y \cdot \frac{\delta h}{\delta y}; \text{ and } q_z = -K_z \cdot \frac{\delta h}{\delta z} \quad (1)$$

where K_x , K_y , and K_z are hydraulic conductivities along the x, y, and z direction (LT^{-1}); h is the hydraulic head (L); and q_x , q_y , and q_z represent the volumetric flow rate per unit area (L). The groundwater flow equation of MODFLOW

(2) is:

$$\frac{\partial}{\partial x} \left(K_{xx} \frac{\partial h}{\partial x} \right) + \frac{\partial}{\partial y} \left(K_{yy} \frac{\partial h}{\partial y} \right) + \frac{\partial}{\partial z} \left(K_{zz} \frac{\partial h}{\partial z} \right) - W = S_s \frac{\partial h}{\partial t} \quad (2)$$

Where K_{xx} , K_{yy} , and K_{zz} are values of hydraulic conductivity along the x, y, and z coordinates (LT^{-1}); h is the potentiometric head (L); W is a volumetric flux per unit volume and represents sources and/or sinks of water (T^{-1}); S_s is the specific storage of the porous material (L^{-1}); t is time (T); $\delta h / \delta x$, $\delta h / \delta y$, $\delta h / \delta z$ are the respective spatial hydraulic gradients; and $\delta h / \delta t$ is the temporal derivative of the hydraulic head. Simulations with steady-state conditions do not consider the specific storage term of equation (2) as inflows and outflows are constant through time. Solution of these equations in Modflow is carried out through the division of the model domain into a rectilinear cell grid setting according to layers, rows and columns that extend through each layer. Hydraulic heads are computed at the center of each model cell and aquifer properties are considered uniform within each individual cell (Kernodle et al, 1995).

3.5.3 Hydrological model setup / Model framework

ModelMuse (Winston, 2009) was used to prepare model inputs for MODFLOW to simulate groundwater flow and investigate drain-aquifer relationship. Our model uses MODFLOW-2005 and implements two other packages, Drain (DRN) and Recharge (RCH).

First, grid discretization was modified several times. The DEM pixel elevation changes were large relative to the watershed size, therefore in order to diminish these jumps, a small grid size of 10 x 10 m was set. The model domain has a regular mesh and a block-centered finite-difference grid, and it covers an area of about 7 km² with a horizontal uniform cell size of 10 m in both the x and y directions, which covers a total of 302 columns and 229 rows. There is a total of 1030300 active cells in the model domain.

Vertically, the model domain was divided into three main geologic layers which were subsequently discretized to a total of 25 grid layers that allowed a good level of detail and analysis. The first two main layers were set up as unconfined layers and the basement or bedrock as a confined unit. Geologic layer thickness and hydraulic conductivities were estimated from exploration drill-hole data across the watershed (see section 3.4).

Groundwater recharge into the saturated zone occurs through infiltration either of rain or snowmelt, outflow from the zone is drained from the ephemeral creek at the mouth of the watershed. No-flow boundaries were assumed around the perimeter of the watershed. This condition is assumed along the mountain ridges which would coincide with the surface watershed divide. This assumes that no cross-basin groundwater flow occurs. Even though this may not be a robust assumption, particularly on the downstream end of the watershed, it opens a potential area for future investigation. Recharge and the outflow exiting the basin will be considered as the water source and sink, respectively, for the area. Recharge has been estimated from meteorological data (see section 3.3) and is distributed evenly across the model as a specified flux into the top active cell. The MODFLOW Recharge package was used to simulate this input.

The small ephemeral creek that covers a small portion at the outlet of the basin was simulated through the MODFLOW Drain package. The drain is designed to remove surplus water at the ground surface and it is assumed that creek water source is entirely groundwater baseflow.

3.5.4 **Model recharge**

Precipitation for the steady-state simulation was considered as an average of ten years of estimates from Pelambres Mining data (1993-2013). This value, (9.81E-09 m/s) includes both rainfall and snowmelt (Figure AA). Recharge in the transient simulations was incorporated monthly according to field data. Monthly rainfall and snowmelt from 2013 to 2019 was added to create a total of 84 monthly values (i.e. stress periods). Figure 3.8 depicts the total recharge rates considered.

3.5.5 **Model parameters and calibration**

As a first step, a steady-state model was created for Altar valley to set the initial conditions and hydraulic heads for the transient simulations. The percent discrepancy values for the MODFLOW steady-state simulation results were not higher than 0.05, aligning with Anderson (1993) who states: “an effective numerical simulation is tested when the percent discrepancy result comes to 0 or is less than 1 percent”.

The steady-state simulation for the base scenario (Table 3.3) was developed by tuning model inputs and gridding to obtain a robust solution with minimal numerical errors. Then, the calculated hydraulic head values from the steady-state simulation were used as initial conditions for the transient model, which simulated transient flow conditions for the period 2013-2019.

Drain conductance parameters were aligned with the hydraulic conductivity of the upper layer. The small creek in Altar is very small, therefore the drain elevation was set at 0.30 m below the DEM, a width of 1 meter and hydraulic conductivity of 0.1 m/sec with a total length of 246 m.

Model calibration was intended to be carried out with field data, but unfortunately the temporal and spatial distributions of head and streamflow data were insufficient to achieve a robust calibration. Therefore, a sensitivity analysis was undertaken to understand and gain insights into the groundwater system in the area.

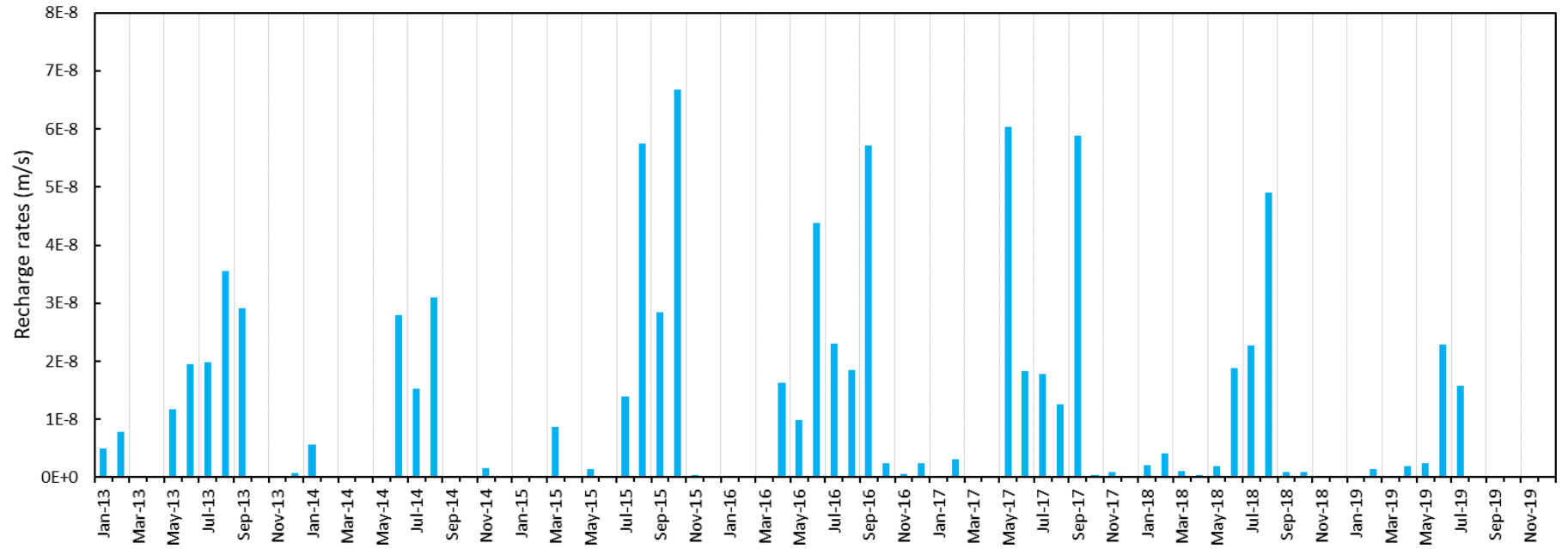


Figure 3.8: Recharge rates for the transient simulation. Each month represents a stress period of a total of 84.

Hydraulic parameters were unknown in the area. Therefore, studies in similar high-elevated mountains were considered and reference values were extracted from Clow et al. (2003), where they estimated hydraulic conductivities for an alpine catchment where alluvium, talus slopes, and bedrock outcrops dominate the landscape. Then, K was adjusted to obtain a base case scenario that best approximated head measurements observed in the field. The hydraulic conductivity distribution for the base case scenario is shown in Figure 3.9.

Horizontal hydraulic conductivity (K_x) was changed through multiple simulations. Vertical hydraulic conductivity (K_y) was set equal to K_x and K_z at one tenth K_x ($K_z=K_x/10$).

Different flow packages and solvers were tested to reach convergence. Best results were achieved using the 'Layer Property Flow package'(LPF) and the solver 'Preconditioned Conjugate Gradient package'(PCG).

As a measure to corroborate model results, head outputs were analyzed. A series of 4 head observation wells (HO) were positioned within the model domain (Figure 3.10). However, only one well (P5, Figure 3.1) at the outlet of the basin allowed comparison with field measurements. This well is the only one that has a consistent record from 2016-2020, whereas P1 (Figure 3.1) has an intermittent record (Figure 4.6 A-B), and is also near a rock glacier, which is not simulated.

The model was initiated from January 2013 and run with monthly stress periods until December 2019. A total time lapse of 7 years was simulated, with 84 monthly stress periods. Time steps within periods were adjusted to minimize convergence errors. Such errors were predominantly occurring due to lack of or low recharge inputs.

Parameter	Alluvium and fractured bedrock	Bedrock layer
Layer type	Convertible	Confined
Specific storage	1E-5*	1E-5*
Specific yield	0.2*	
Layer thickness	Alluvium: 0 to 60-80 m Fractured bedrock: 240 to 360 m	270 to 360 m
Drain conductance	$((K_{\text{drain}} * \text{Drain_width}) / \text{Drain_sed_thickness}) =$ 0.1	

Table 3.3: Parameters used for the base case scenario. (*) Values according to Fetter, C. W. (1994).

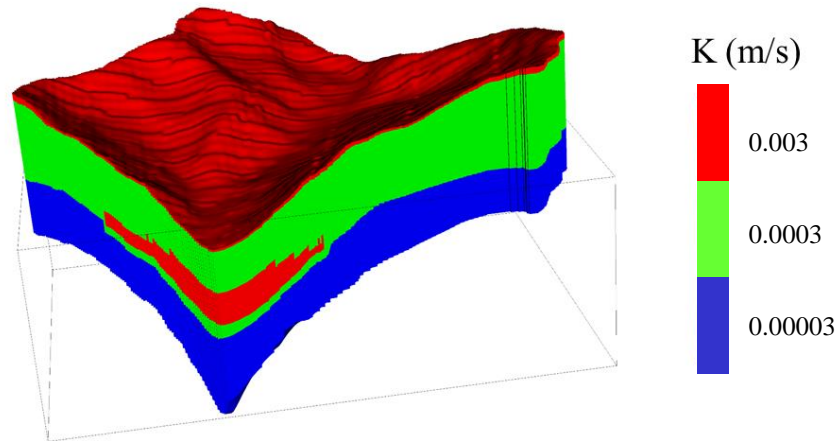


Figure 3.9: Hydraulic conductivity distribution for the base case scenario. Three main layers and two different zones (converted to one) with a higher zone than surroundings. These zones have always a K similar to the surface according to the scenarios.

3.6 Sensitivity analysis

In order to answer the research questions and explore watershed sensitivity response to model parameters, four different scenarios were considered: the base case, two different K values (Table 3.4), and a reduction in recharge. The scenarios chosen consider as a reference the base case, they were: 1) 10x higher hydraulic conductivity, 2) 10x lower hydraulic conductivity, and 3) a decrease of 15% in precipitation considering sublimation, evaporation, and climate change. This latter scenario assumed that 10% of the snowfall sublimates and all rainfall during the summer evaporates. Several studies in the Andes state that sublimation is directly related to elevation, strong winds, and radiation (Ayala, et al., 2017; Corripio, 2003; Réveillet et al., 2019). At low altitudes snowmelt prevails over sublimation, but as the gradient increases, sublimation overcomes snowmelt and is significant above an elevation of 5000 m.a.s.l (Figure A.9). Therefore, recharge rates in the model did not consider any rainfall during the summer and the sublimation percentage was subtracted every winter season from the total snowmelt. The other 5% reduction in recharge corresponds to climate change forecasts. Results from a downscaling model show an average negative trend in precipitation of $-4.7\% \text{ decade}^{-1}$ (Souvignet et al., 2010) (See section 1.3). Although our weather dataset covers seven years, we considered a reduction of 5% in precipitation.

Simulation outputs were compared and assessed to understand responses of the system to changes in the model parameters. Monthly drain budgets and daily observation heads during transient simulations were assessed. Model results were also analyzed with MODPATH. MODPATH (Pollock, 2016) is a particle tracking post-processing model that uses MODFLOW outputs. This program computes flow paths

and transit times for water particles moving through the groundwater system. This was applied to reverse particle tracking for Altar Creek and Piezometer 1 (Figure 3.1).

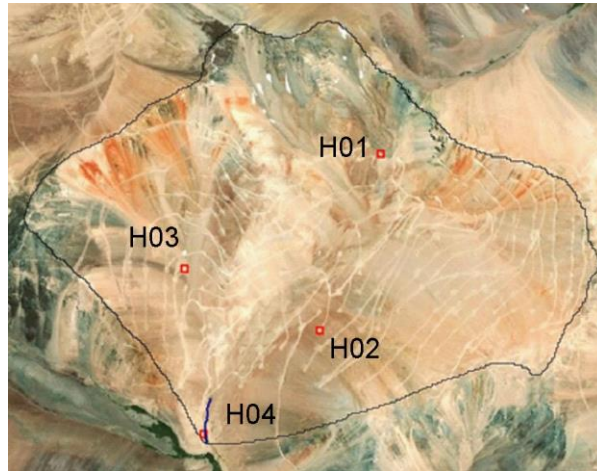


Figure 3.10: Location of the model observation wells (red squares).

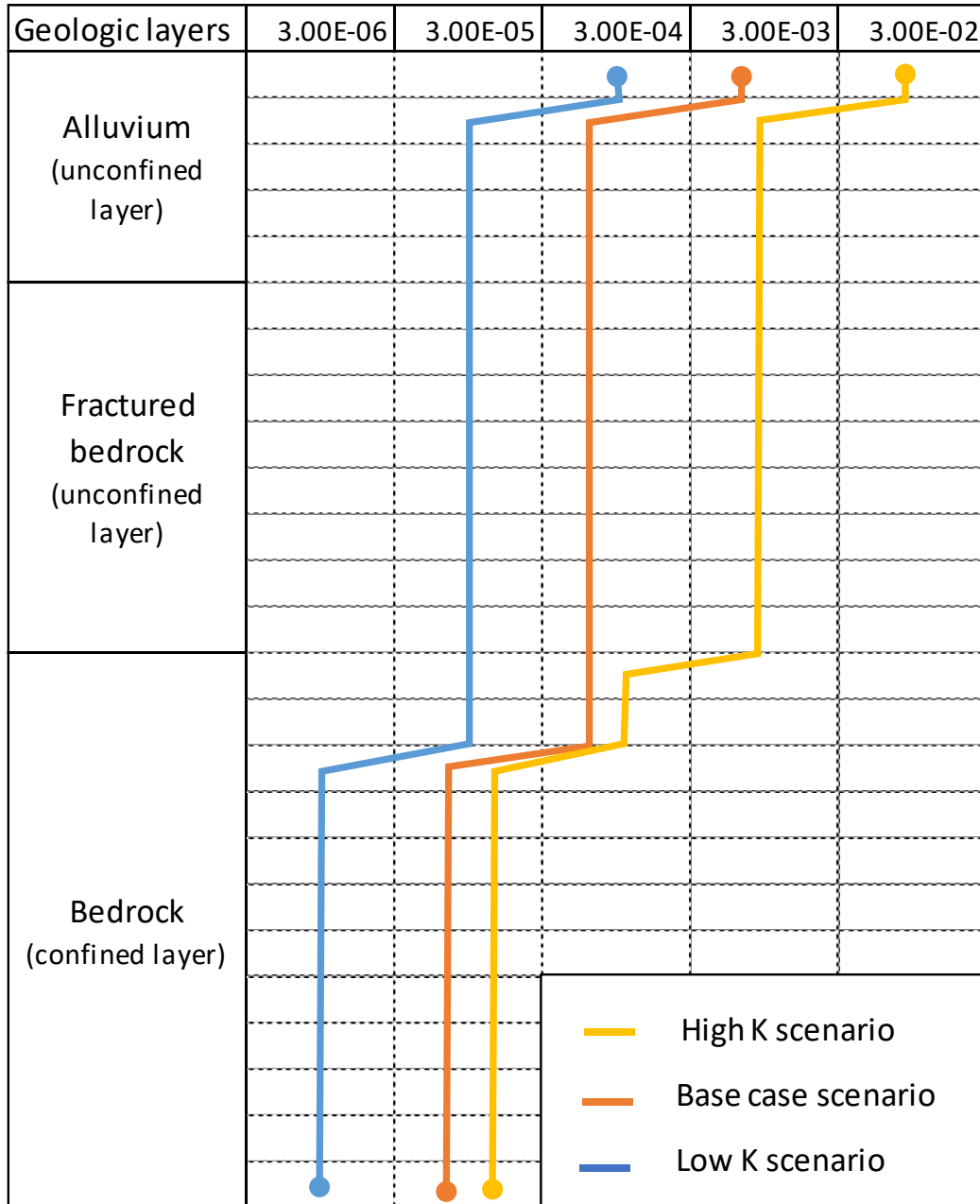


Table 3.4: Plot of vertical K values versus layers. Each row represents a model layer (25 total).

Chapter 4

RESULTS

4.1 Ice and water sampling.

Tritium activity in the ice samples ranged from undetectable (<0.09 TU) to 0.17 TU, indicating little or no contribution of post-bomb precipitation (post-1963) (N. Sturchio, personal communication). Figure 4.1 shows the tritium activity with a peak in 1963 at about 50 TU, which would mean that precipitation from that time would have a tritium activity of about 2 TU today. Pre-bomb precipitation had roughly a tritium activity of 5 TU; therefore, precipitation from 1950 would now have a tritium activity of 0.2 TU or less. According to these scenarios and results, the ice samples taken at QDM may have formed from precipitation older than about 65 years. In the case of groundwater samples from P5 and Rio Tinto 1 wells (Figure 3.1), tritium contents were <0.2 TU, indicating mean subsurface residence times greater than 65 years (<1950).

Sulfur hexafluoride (SF_6) results suggest a mean residence of time of about 20-30 years in P5 well (Figure 3.1), which is consistent with a considerable storage time for water in the ground while Rio Tinto 1 well, groundwater has a mean residence time of 0-10 years. However, from tritium analyses, both P5 and Rio Tinto 1 waters showed tritium <0.2 TU, implying a recharge time older than 65 years (Sturchio, 2018). This mismatch in results likely indicates contamination of water samples with excess air during sampling making the samples seem younger for SF_6 . Unfortunately, the depth of the Rio Tinto well is unknown, whereas P5 has a total depth of 15 m located within the alluvium layer at that point.

Results from stable isotopes of groundwater and surface water could not distinguish between snow and rock glacier ice water sources. This is because the isotopic fractionation of oxygen-18 between ice and water at 0°C is about +3 per mil, which is about the same as the mean difference between ice and water samples from the study area.

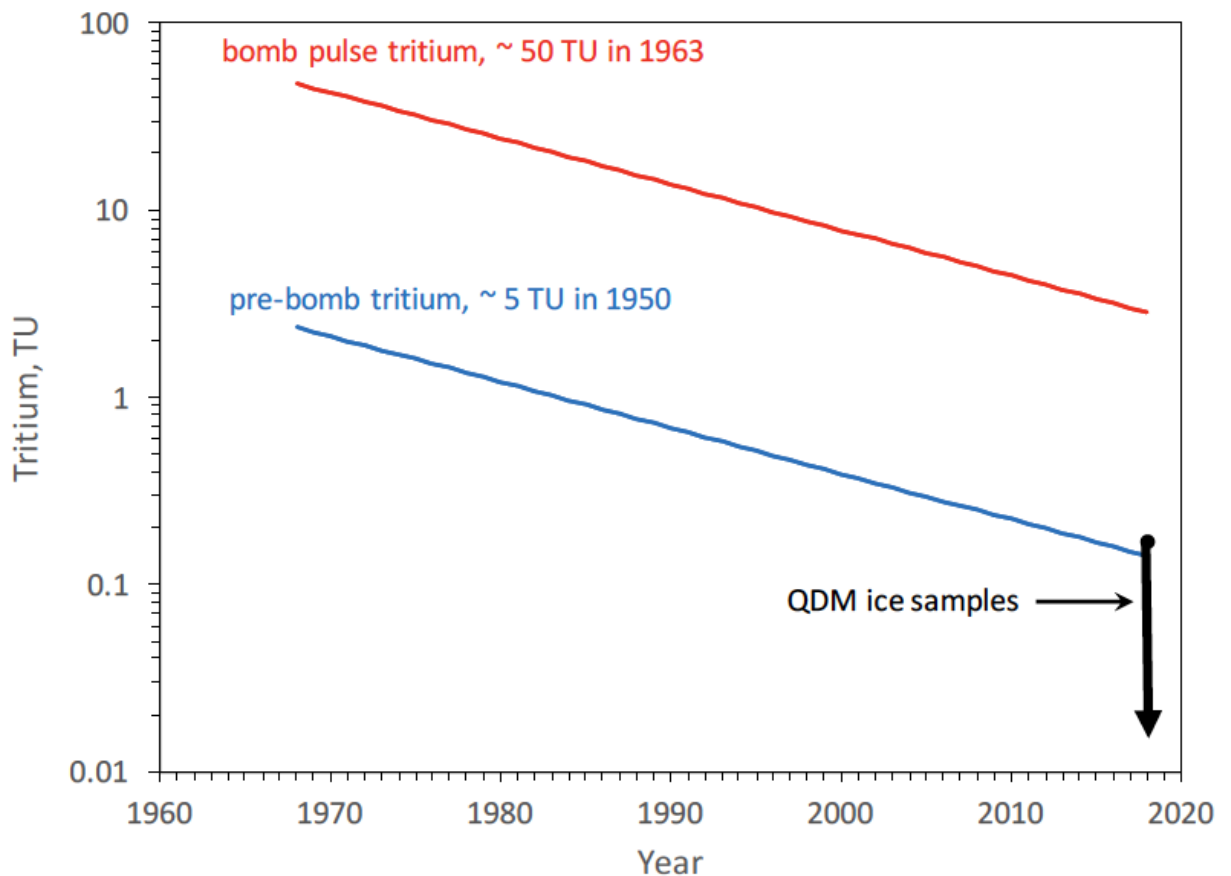


Figure 4.1: Tritium activity (TU) vs. time for water recharged in 1967 during period of peak tritium activity (red) and for water recharged in 1950 with pre-bomb natural tritium activity. Ice samples, as well as groundwater from the P5 and Rio Tinto-1 monitoring wells, have tritium activities consistent with pre-bomb precipitation.

4.2 Weather station measurements

Slightly lower temperatures and less rainfall were observed on the upper station, the latter likely due to the leeward position of the weather station and colder temperatures.

Rainfall is scarce in the area and mostly occurs during the austral summer season (November-March) whereas during the rest of the year precipitation is in the form of snow (Figure 4.3). Average annual precipitation is 30 mm and sometimes barely reaches 5 mm. The high station altitude (3990 m.a.s.l.) coupled with its leeward position may reduce ability of the pluviometer to accurately catch rainfall events, especially with high winds. This is further complicated when measuring meltwater from snowfall events. On the other hand, the lower station shows regular behavior between rainfall and snowfall. While rainfall occurs mainly in the summer during November through March, snowfall events occur during the winter months of July through October. Rainfall events observed at the lower station during the snow season may be due to its lower elevation and slightly higher temperature or to the partial melting of the snow from the pluviometer; these events were not considered into the recharge estimates.

Snow measurements are recorded solely at the lower station near the mining camp (Figure 4.3B). Snow storms can occur from May till October and snow accumulation can last as long as October or be completely melted by July (i.e. season 2019). Within the timespan covered by the sensor there were three major seasons with important snow accumulations (2015-2016-2017), in which snow height reached 1 m on the site, but since then records show a decrease in precipitation shortening the snow season either in time or snow accumulation.

Temperature (Figure 4.2) shows slightly higher values on the lower station compared to the upper site. Unlike the 2016 summer season, in which the upper station showed cooler than average temperatures, no temperature trends were observed. The measured range in temperature varies from -15°C to 15°C .

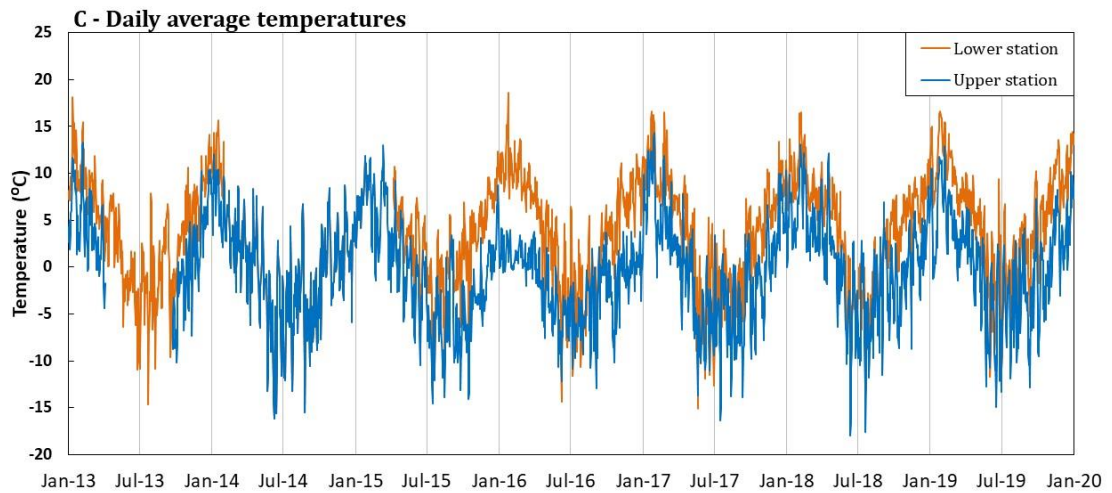


Figure 4.2: Weather station temperature data from January 2013 to January 2020 (gaps in the data exist).

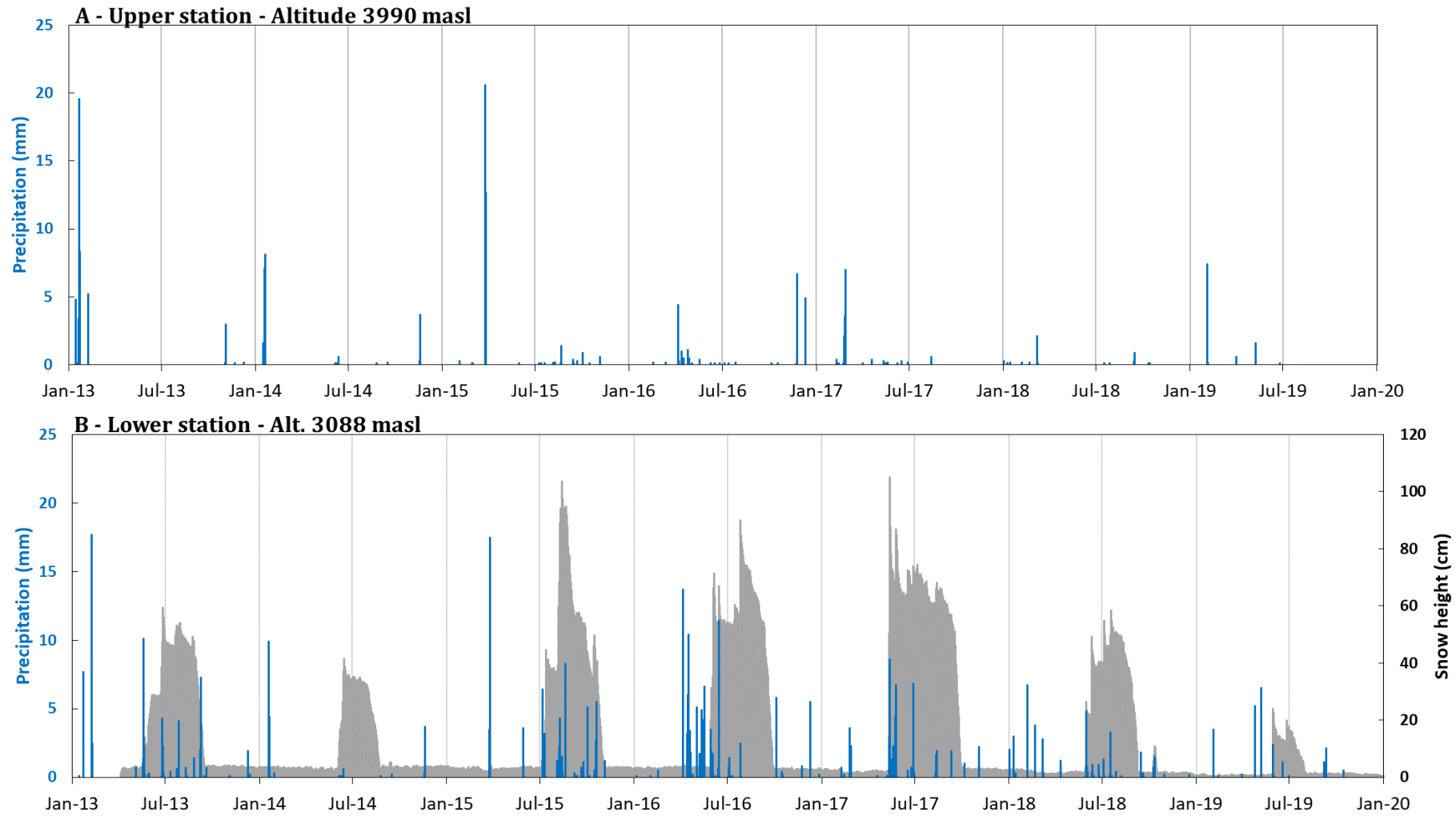


Figure 4.3. Weather station data from January 2013 to January 2020. A: Precipitation data from upper station. B: Precipitation (blue bars) and snowfall height (grey shadow) from lower station.

4.3 Weir data

After a year of recording (from April 2019 to March 2020) the data were collected and analyzed during summer 2020. Unfortunately, the low precipitation that prevailed in the region for several seasons resulted in low or non-existent flow, therefore only a few measurements were recorded (Figure 4.4). Most measurements are concentrated during two months in fall (April and May 2019) where flows are commonly low. There are few measurements during the melting season (September 2019) where the record shows up to seven centimeters of water over the v-notch. During the summer the weir remains dry and no measurements are recorded even prior to the same period in 2019. The accuracy of this weir could be questioned, especially during the last months since by March 2020 it had shown significant signs of erosion and cracks on its structure. Thus, discharge measurements have been affected. The water acidity, which was not considered when choosing the material, deeply eroded not only this weir, but also others located downstream (Figure 3.3). A relationship between stage and discharge was computed at the weir (Figure 4.5). Most of the discharge over the weir was less than three centimeters and occurred during early fall.

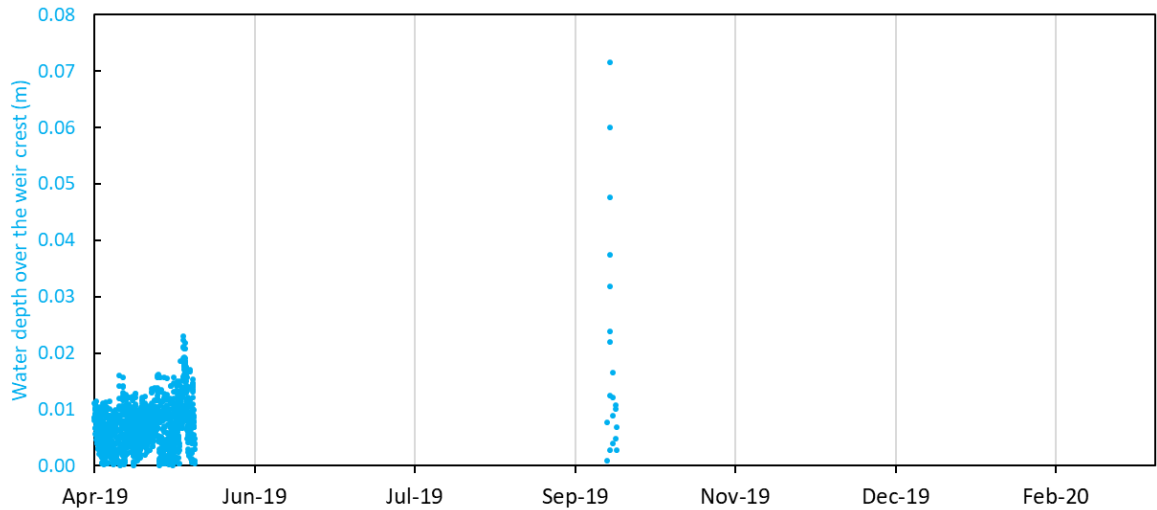


Figure 4.4: Water depth over a v-notch weir at the outlet of Altar watershed from April 2019 to March 2020.

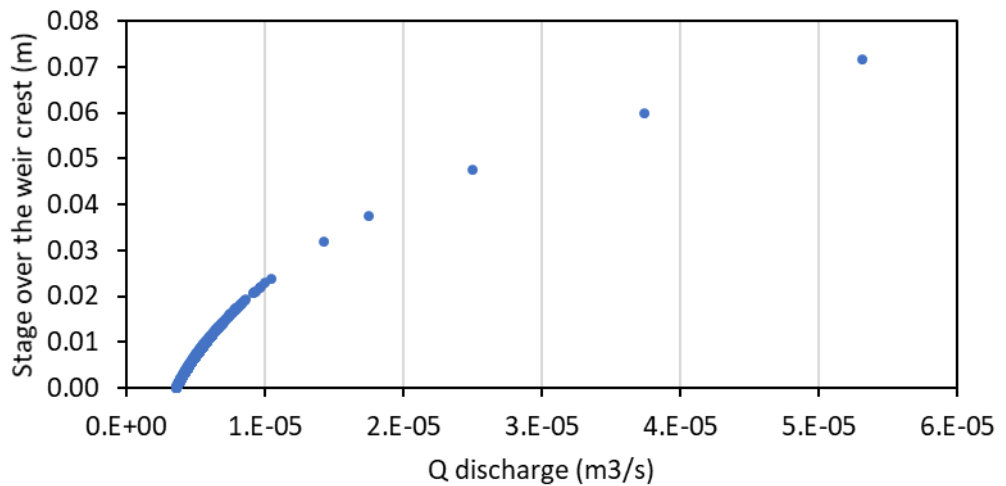


Figure 4.5: Creek water stage versus discharge for the weir at Altar watershed.

4.4 Water wells

At the highest point on East Altar and directly below the only rock glacier on the valley, the water table elevation exhibits seasonal trends with four characteristic peaks that occur during the spring snowmelts (P1, Figure 4.6A). At that time, due to warmer weather, the snowpack that grew over the winter starts to melt, recharging the

groundwater. Melt from the rock glacier may also contribute to groundwater recharge in this area. After November-December, groundwater levels declined throughout the summer, when few rain events occurred and snow and glacier meltwater decreased. This behavior ends with the next spring season (September-October-November) when the cycle resumes again. Because this site is particularly high in elevation, the temperatures become cool after March (fall) and the site receives less solar radiation (Figure A.7A). A significant head drop occurs during spring 2019, which likely is due to the poor previous snow season. Gaps in data are the result of groundwater levels dropping below the logger elevation. However, in March 2018, the logger was relocated deeper, close to the bottom of the well. Despite this deeper location, the water table appears to keep dropping beyond the pressure transducer depth. Due to the high elevation of the water table at this location, we suspect that the heads are maintained within a perched aquifer which likely appears and disappears annually. Temperatures are plotted in yellow in Figure A.7A and show a range between 1.5 to $\sim 0.25^{\circ}\text{C}$ from winter (June through August) to summer season (November till February). These changes in temperature were expected to be the opposite, with water temperatures associated with warmer air temperatures and high solar radiation during the summer. These observations can be explained by the pressure transducer being exposed to air during the winter and then measuring the thawed recharge water during the spring.

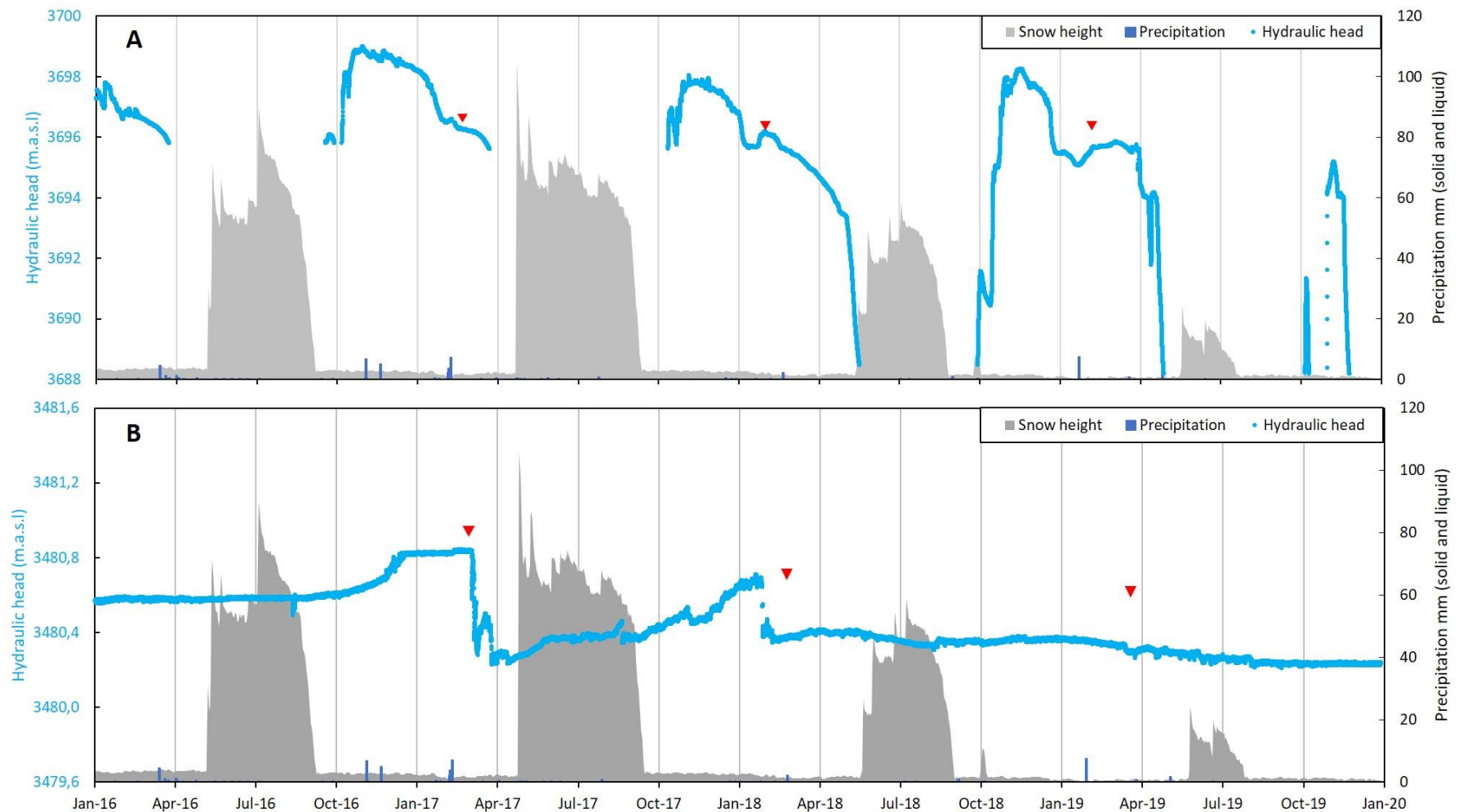


Figure 4.6: A: Water table vs precipitation for piezometer P1. Elevation 3705 m.a.s.l. B: Water table vs precipitation for piezometer P5 Elevation 3480.4 m.a.s.l. Time-lapse 2016-2020. Red triangles indicate data logger removal and the start of a new data long-term deployment. Gaps in data indicate lacks of measurements. Snow height data from lower weather station.

Downstream and next to the headwaters of Altar Creek another sensor recorded heads in the subsurface (P5, Figure 4.6B). The water table (blue line) showed a strange pattern at during the first two seasons. During 2016-2017 the groundwater table first increased and probably groundwater overflowed the casing (time of constant head during the months around January 2017, and then suddenly decreased. The steep, but not instantaneous, decline in the water table is not completely understood. Data were processed and checked for errors or whether personnel removed the logger, but nothing has been found to explain this jump. Although the logger is located 15 meters deep, it is possible that there was freezing in the borehole, and that the head drop was due to melting but this can be arguable as well. Subsequently, seasonal changes were smaller and artesian conditions were not observed in the head record. Groundwater temperature (Figure A.6) depicts a regular cycle with increases from ~4.5 to 5.5°C from spring to summer in accordance with snowmelt season. The record over time shows a slight increase in the minimum water temperature over time.

Another pressure transducer (P6, Figure 4.7A) is located on the alluvial fan at the mouth of Altar creek. The record extends from 2016 to 2018 and then from April 2019 to 2020. More than a year of data between 2018 to 2019 was lost when the logger fell to the bottom of the well. Temperature shows spikes in all seasons (Figure A.7.B). Downward trends could be interpreted as snowmelt processes, which bring fresh cold water to the system, whereas upward trends may represent greater water circulation and thus a warmer temperature. Regarding water table elevation, two peaks stand out whose timing matched the beginning of the spring season, highlighting the influence of snowmelt processes on the water table. The two spikes observed become

smaller from year to year, which could imply less snow availability and thus less recharge into the system.

The last two loggers are located next to the La Pantanosa River that is the main surface water discharge of the area. P7 (Figure 4.7B) is positioned upstream of the Altar Creek confluence and mining camp, whereas P8 (Figure 4.8) is downstream some kilometers below the camp and the Altar Creek confluence. The downstream logger did not show large changes either in temperature or water level elevation as it is an artesian well. However, the upstream well (P7, Figure 4.7B) displayed a continuous temperature decrease from February until September then a steady increase during summer months in accordance with seasonal patterns. The observed seasonal temperature increase was about 6°C. Minimum observed temperatures increased with time throughout the record, whereas maximum temperatures remained constant (Figure A.8). The water table showed a rising pattern and a wide bell shape (2016), which became smaller over time and where melting was delayed from April 2016 to August 2018. Such changes are interpreted as a combination of rainfall events and snowpack melting during 2016 (Figure 4.7B) and then a delay in snowfall and smaller snowpacks for the last two seasons (2017-2018). Thus, these changes brought diminishing recharge and less groundwater discharge to the hydrologic system that is reflected in the groundwater levels.

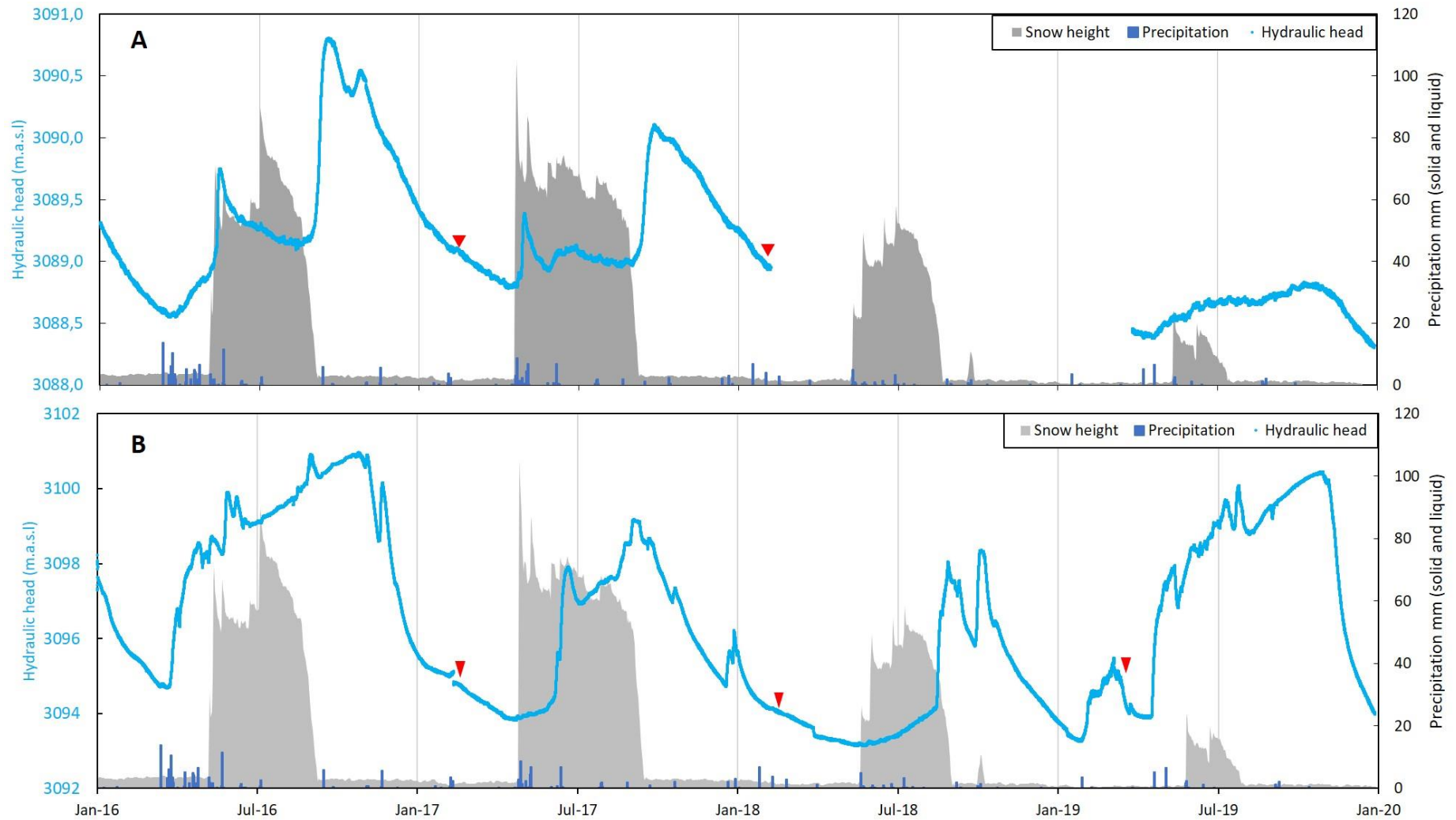


Figure 4.7. A: Water table and precipitation for piezometer P6. Elevation 3105 m.a.s.l. B: Water table vs precipitation for piezometer P7. Elevation 3103 m.a.s.l. Red triangle indicates data logger removal and the start of a new data long-term deployment.

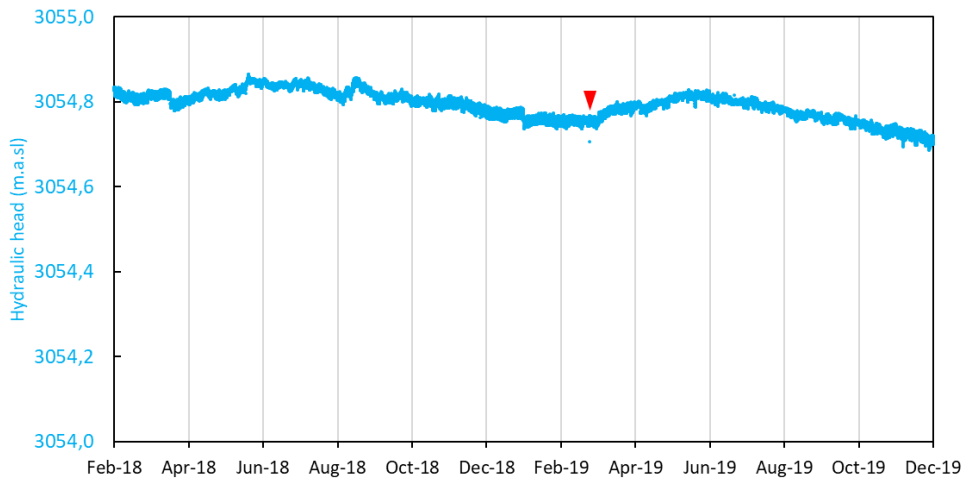


Figure 4.8: Water table vs time for piezometer P8. Time-lapse 2018-2019. Elevation 3054 m.a.s.l. Red triangle indicates data logger removal and the start of a new data long-term deployment.

4.5 Snowpack distribution

Snow height distribution throughout the season changes as it can be observed in Figure 4.9. Peaks in accumulation reached 1.05 m the during 2015 and 2017 winter seasons. Most of the records show that first accumulations usually occur in May, with some delayed as late as July. First accumulations are usually within 0.20 cm although records show up to 1 meter for the first snowfall. Peaks within the records represent snow storm events, which contribute to the snowpack vertical growth. The same plot displays average temperatures for the years covered. Temperatures are around 4°C at the beginning of the winter season and drop up to -6°C during June and July, considered the coldest months in the austral hemisphere. Overall snowpack does not show negative/melting trends under 0°C but as the season continues, temperatures over -2°C make the snowpack more prone to melt and sublimate. By the end of September and beginning of October all the snowpack has completely melted which is

accompanied with temperatures that rise back up to 4°C by November. Exceptions are observed and the 2019 winter season depicts the shortest extension and lowest snow height compared to previous seasons.

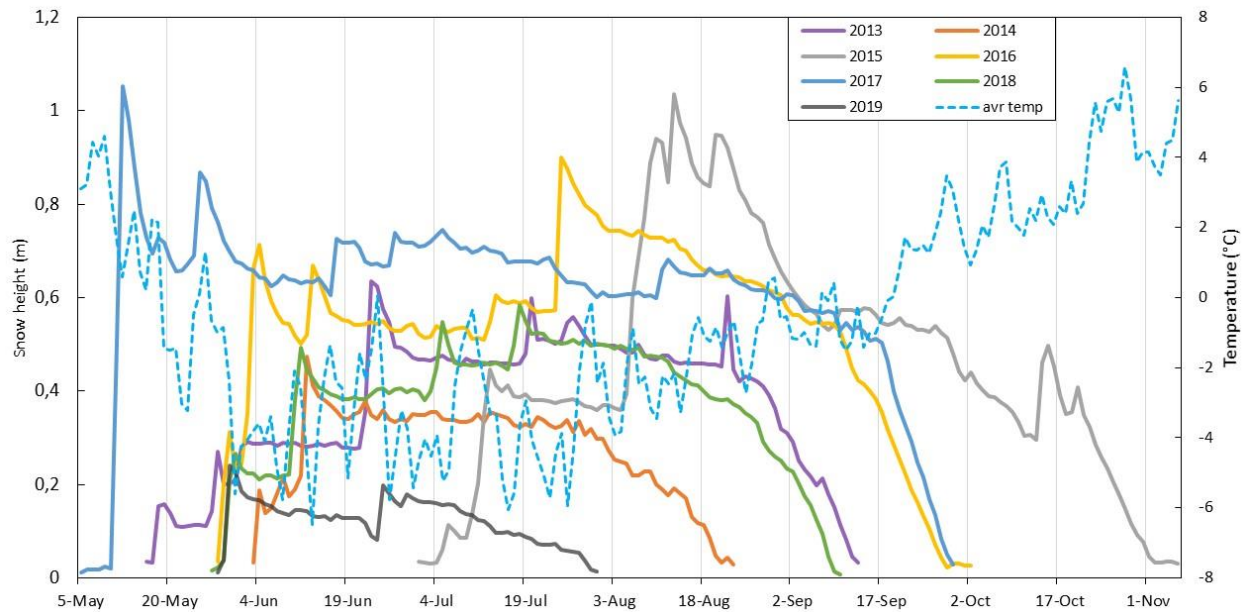


Figure 4.9: Snow height distribution and average temperature from 2013 to 2019.

4.6 Altar rock glacier contribution

In order to obtain estimates of the recharge contribution of the Altar rock glacier, we computed estimated minimum recharge rates beneath the rock glacier for the four recorded years. As it is observed in Figure 4.6A, clear head increases are observed for the four years, and we used the 2018 and 2019 data for analysis since the sensor was deeper in the well and therefore the record is more complete. We computed the annual head rise for each year and considered a conservative value of porosity of 0.2 (Morris and Johnson, 1967). Head rises and rock glacier recharge rates per year are in Table 4.1. The head rise times porosity is a conservative value of added recharge beneath the glacier because 1- the actual head rise is greater than measured since the sensor is dry at the beginning of the

season, 2- the value of porosity is likely higher than 0.2, and 3- the calculation assumes that there is no lateral flow away from the point of recharge, which is unlikely.

Computed rock glacier point and volumetric contributions were obtained. Considering the glacier area of 65,400 m² computed by Shumlich (2018), we estimated the volumetric contribution of water from the rock glacier per year. In the same line, we computed annual recharge rates for the watershed area (4,121,200 m²) and analyzed the annual rock glacier point contribution and overall contribution to recharge. The conservative point estimates of rock glacier recharge of 1.7 and 1.1 m/yr for the two years are much greater than the 0.3 m/yr for the overall watershed recharge. Multiplying by the area of the watershed, we obtain the annual volumetric contribution of the rock glacier. Despite only having 1.6% of the watershed total area, the rock glacier contributes at least 10% of the overall recharge. Although these results are rough estimates, they give a clear indication that recharge contributions from rock glaciers are locally important and non-negligible, though the overall impact on watershed-scale recharge depends on its relative area in the watershed.

Year	Head rise dh (m)	Time duration (days)	Recharge rate beneath rock glacier (m/yr)	Rock glacier point contribution (m/yr)	Volumetric rock glacier contribution (m ³ /yr)	Volumetric watershed recharge (m ³ /yr)	Rock glacier contribution to the overall recharge (%)
2018	9.8	48	2	1.7	1.1E+5	1.1E+6	9.9
2019	6.8	7	1.4	1.1	6.8E+4	4.8E+5	14.3

Table 4.1:Altar rock glacier contribution estimates from 2016 to 2019.

4.7 Groundwater simulation results (Base case scenario)

Steady-state simulation results showed heads of 3472.7 m.a.s.l. and 3478.3 m.a.s.l. as the lowest and highest heads respectively, of the model domain.

Heads in the field for P1 vary widely from 3688.6 up to 3698.9 m.a.s.l. (Figure 4.6A, see section 4.4). The location of this sensor, next to Altar rock glacier, shows a strong influence of the snowmelt season which usually extends from August to October. Once the snowpack melts, heads slowly start dropping during the summer until the next thawing season. Simulated heads with ModelMuse were lower by 204.5 m (Figure 4.10A). This discrepancy is likely because the heads in P1 are recharge from the rock glacier, and likely within a perched aquifer. Since recharge is applied directly to the water table in MODFLOW, and since the recharge from the rock glacier is incorporated, we do not expect the simulated and measured heads to match in this location. The average simulated head is 3478.8 m.a.s.l. with a maximum head increase during spring 2015 when heads jump near 3 m within a four-month timespan. Simulated heads increase near 3, 2, 2.4, and 1.3 m are observed for the seasons 2015, 2016, 2017, and 2018 respectively within 3 to 5 months. Whereas observed heads increases are larger and shorter in time. Increases of 3, 2.4, and 9.8 m are observed for 2016, 2017, and 2018 respectively within 1 and 2 months. This lack of representation between observed and simulated heads could be due to the existence of a perched aquifer that allows heads to stay high during times of high recharge, and likely disconnected from the groundwater system.

On the other hand, heads in the field for P5 are shallow and close to the surface and in some cases above it (artesian conditions were observed), average head is 3480.44 m.a.s.l. (Figure 4.6B and A.4A). In this case, the observed and simulated heads were taken at the real screen depth (15 m). Simulated values are on average 3474.8 m.a.s.l. (Figure 4.10B). However, it is difficult to directly compare elevations because discrepancies can be caused by the changes in DEM elevation within single MODFLOW

cells. In order to more directly compare simulated results to observations, we consider the difference between the head at the well and the water level at the stream outlet. The difference between the simulated heads and DEM stream elevation are smaller (~1.7 m) than the difference observed in the field (~6.7 m). Furthermore, DEM maximum elevation difference over the area of well pixel is 2.9 m. Despite the existence of this gap, it is though that a small average difference of 5 m is reasonable between observed and simulated values since there are multiple sources of error, including steep gradients within MODFLOW pixels, errors in the DEM, errors in well and weir location, and errors in surveying the elevation of the well and weir.

Drain outflows were obtained from the model output and then converted to water stage over the v-notch (see section 3.2.2). Discharge varies and are correlated to recharge rates (Figure 4.11). Results show a range of minimum and maximum stage range over the notch of 0.28 and 0.38 m respectively. These values are much higher than the observed water levels, which vary from 0 to 2 cm but unfortunately the weir only took measurements constantly for two months. (Figure 4.4). The measured water levels are consistent with visual observations at the site. The discrepancy between measured and simulated values indicates that either estimated recharge rates are more than an order of magnitude too high or that there is substantial inter-basin flow, which is assumed negligible in the model. Since it is unlikely that recharge estimates are off by so much, we find that inter-basin flow is highly likely in this region.

Most of the peak recharge rates for each season correspond in time with a constant streamflow increase through the snowmelt season, reaching maximum values at the end of the season (Figure 4.11). Responses to recharge are well pronounced and occur quickly for the 2015-2016-2017 thawing seasons, within time spans of 3, 4, and 5 months, respectively. Although recharge does not increase constantly during the mentioned months, discharge increases steadily throughout the snowmelt season and peaks at the end

of the melt. During summer months, although small observed rainfall events occur, decreases in simulated streamflow curve are observed. In fact, decreased discharge trends are always visible from August/October until rates increase again in the next thawing season (Figure 4.11).

In addition to evaluating heads and stream discharge, we assess groundwater ages with Modpath. MODPATH particles are tracked backward from the location of the well screen to the water table recharge location. Analysis from the 175 particles started in well P5 shows that particles flow deep in the system through the intermediate fractured bedrock and they originate up high in the watershed (Figure 4.12). The water flows downward and laterally through the layers to then reach after several hundreds of years the well. Mean travel times are estimated in 143 yr with a std dev of 14.9 yr (Table 4.2). When comparing same parameters in the river, it is clear that overall particles in the river water are younger with a faster mean travel time of 47.7 yr. As it is shown in Figure 4.12, river particles do not get as deep in the system as the well particles do, groundwater surplus that reach the top of the cell gets easier and faster discharged by the drain.

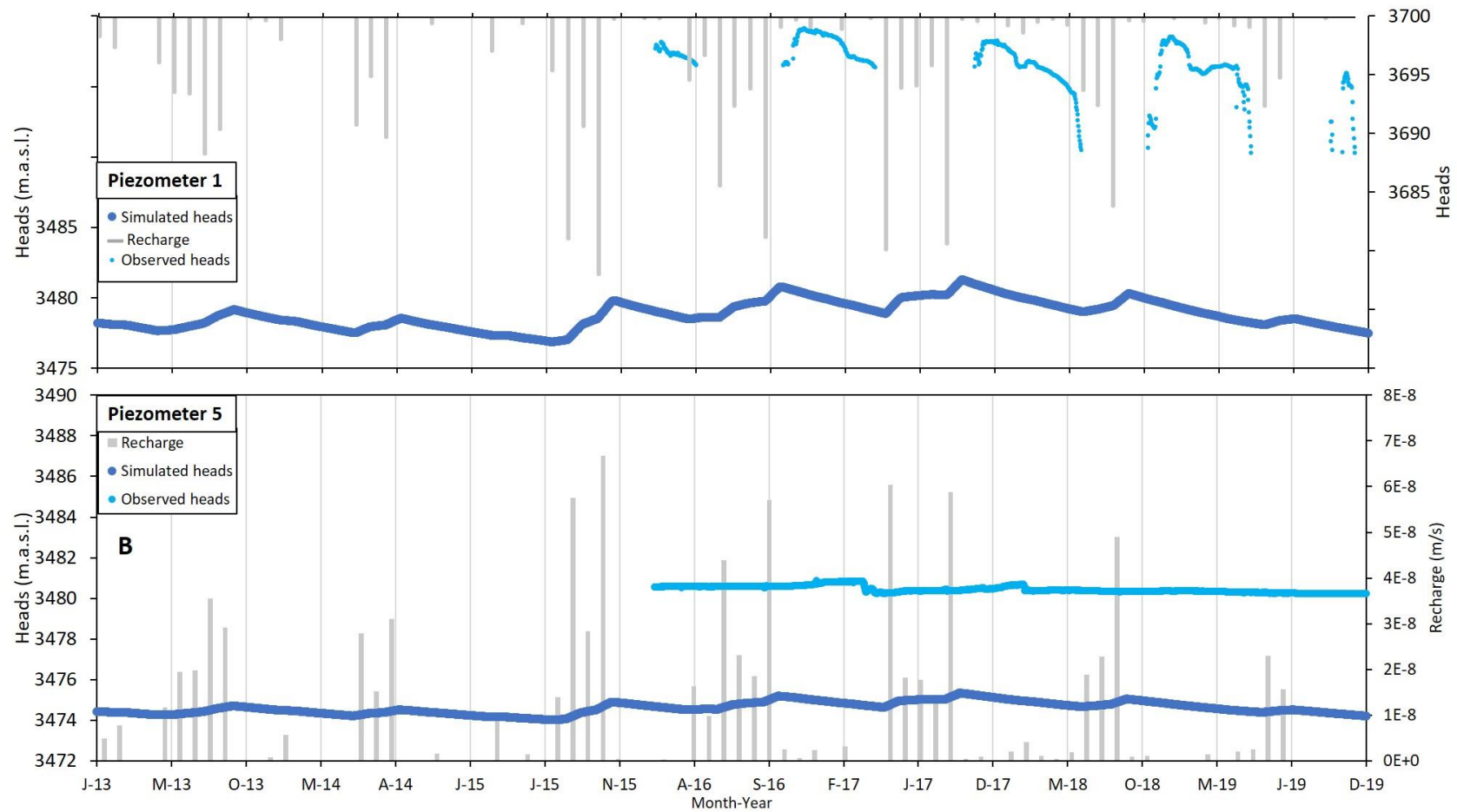


Figure 4.10: Base case scenario results. A: Heads observed and simulated for P1. Note that discrepancy is likely due to perched aquifer conditions and recharge from the rock glacier, neither of which is included in the model. B: Head observed and simulated for P5. Note that head discrepancy is likely a result of inaccurate elevation measurements and DEM data.

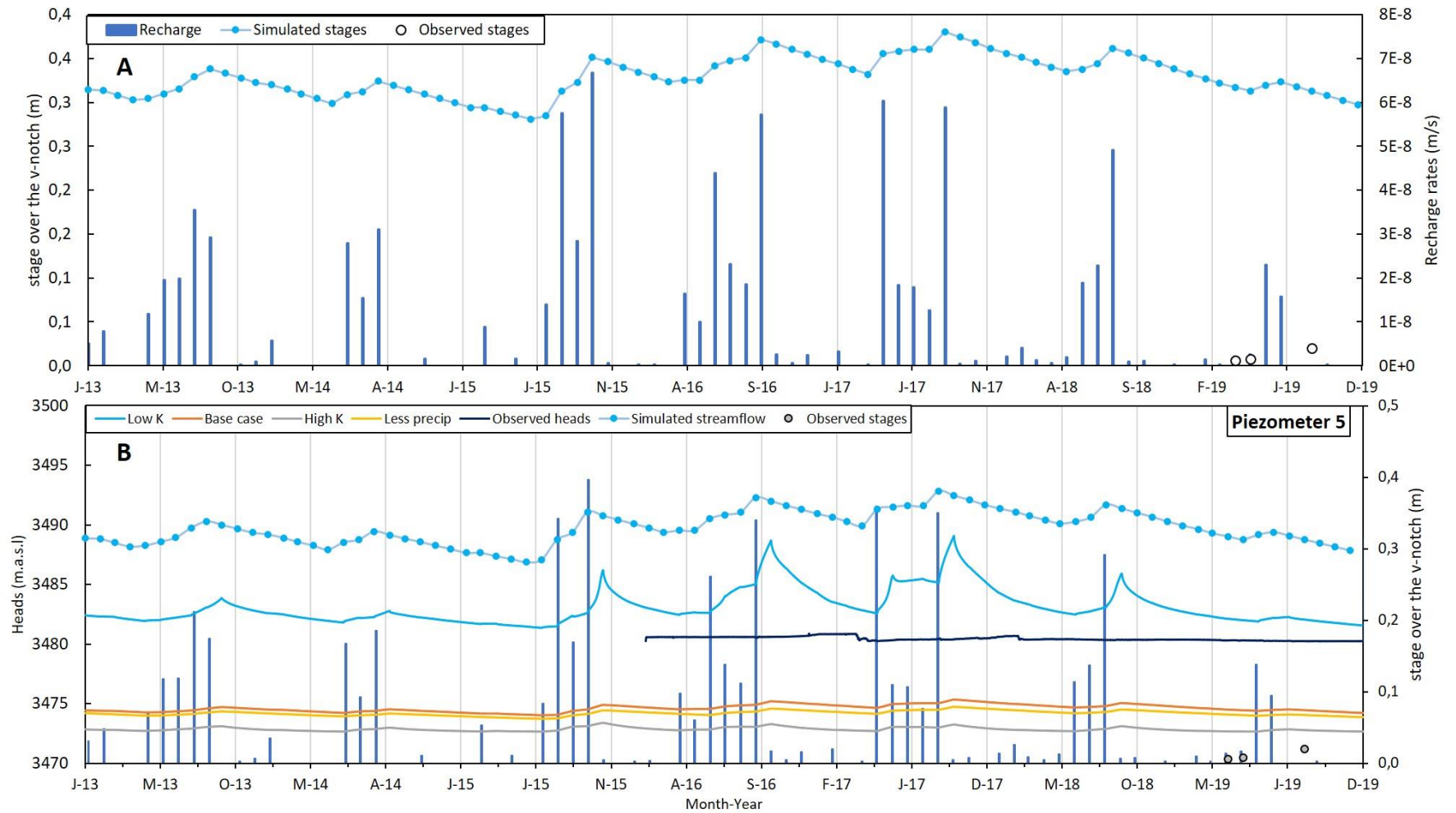


Figure 4.11: A: Base case scenario results. Monthly stream discharge over the v-notch weir vs recharge rates and observed weir levels. B: Simulated daily heads for the transient period at Piezometer 5 at the outlet of Altar watershed. Monthly recharge rates are shown as bars.

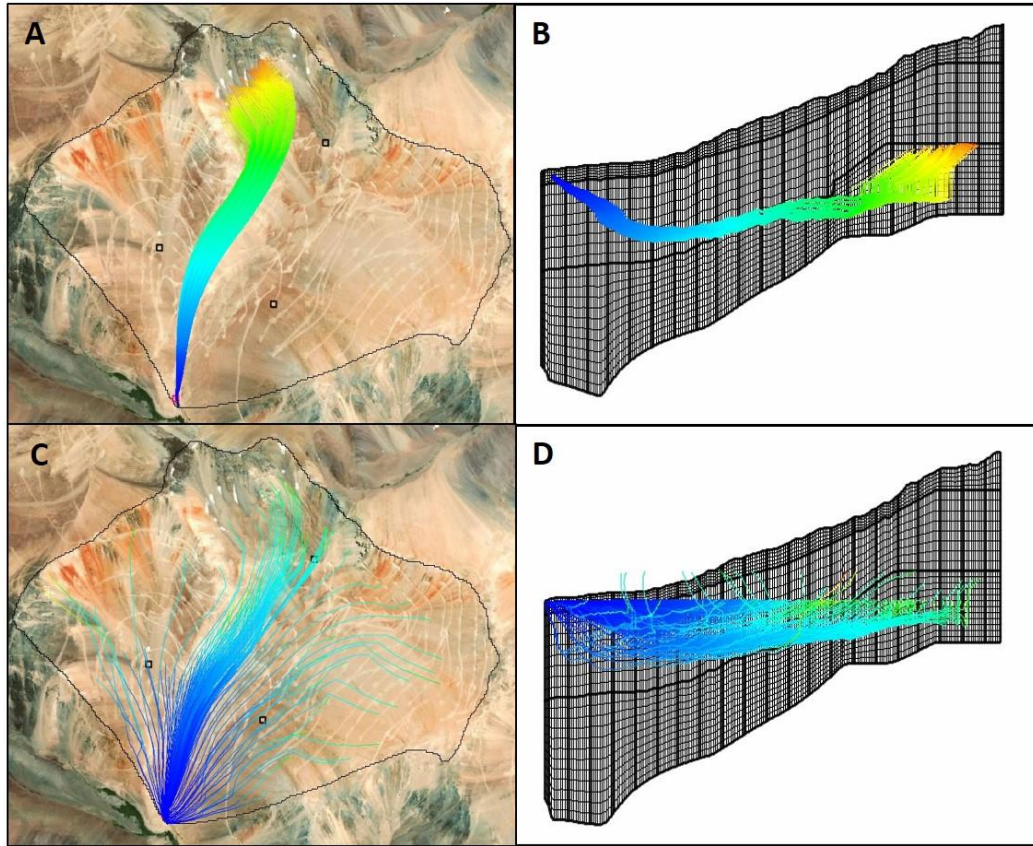


Figure 4.12: Particle tracking to well P5 and the stream. A: Plan view for well particles. B: Side view for well particles. C: Plan view for stream particles. D: Side view for stream particles.

4.8 Model sensitivity

Sensitivity analysis allows for a deeper knowledge of the system through parameter changes. Here we explore how subsurface flow behaves when changes in hydraulic conductivity and recharge are made. Results are observed through simulated water depths at four observation wells indicated in Figure 3.10, drain flow discharge, and flow path.

4.8.1 Hydraulic heads

The following results would compare changes related to the base case scenario. Heads for the steady state and transient simulations for the different scenarios will be mentioned and its trend analyzed.

Figures 4.13 A and B show the simulated heads during the transient simulation for the three sensitivity scenarios and base case in two different locations: high in the watershed next to the rock glacier (P1) and at the outlet of the watershed (P5).

Low K scenario: Results from steady state showed a large head gradient of 3473.1 m.a.s.l. and 3515.7 m.a.s.l. as the lowest and highest heads, respectively. Low and high head records increase by 0.4 m and 37.4 m respectively, when comparing them to the base case, large amplitudes are observed for both P1 and P5 with a low K distribution during the transient period (Figure 4.13). This scenario displays maximum increases of 50 m and 10 m for P1 and P5 respectively. Peaks in heads occur with a lag of 1 month after end of snowmelt season due to measurements are simulated daily whereas recharge is considered monthly. Peaks in heads depend from previous recharge distribution and are reached after 3 to 6 months from the first melting to the end of melting period. Unlike P1, P5 heads are above DEM surface elevation (~6 m), indicating artesian conditions. This is consistent with observations. During summer 2017, artesian conditions existed for approximately 3 months, including a visit when we were able to directly observe artesian conditions (although this record is dubious, Figure 4.6B). For the low-K scenario, heads are on average 40.3 m and 8.5 m higher for P1 and P5, respectively over the base case (Figure 4.13). Results from figure 4.13 display the control that a low K has on heads, when water cannot move fast through a less permeable system, higher gradients are maintained and variability in response to recharge changes.

Higher K scenario: Results from steady state showed a smaller range in heads than a low K, where 3272.6 m.a.s.l. and 3473.4 m.a.s.l. were the lowest and highest heads,

respectively. This latter value decreases by 4.9 m against the base case. Conversely, the high-K scenario results in the lowest heads within the different scenarios and a steadier behavior either in P1 and P5. Amplitudes are smaller than the previous case and they range from 2.2 m for P1 to 0.7 m in P5.

Reduction in precipitation: Heads for steady state range between 3472.7 m.a.s.l. and 3477.5 m.a.s.l. for the lowest and highest heads, respectively. A decrease in maximum heads of 0.8 m is observed against the base case.

Simulated heads for P1 next to the rock glacier and P5 are an average 1.4 m and 0.4 m lower than the base case, respectively. However, overall the general heads follow the same behavior than the base case since both share the same hydraulic conductivity distribution.

4.8.2 **Stream discharge**

Drain outflows display a synchronous behavior with recharge. (Figures 4.14). All scenarios except the one with less recharge have the same precipitation input.

High-K scenarios (Figure 4.14) demonstrate a larger variability between high and low peaks in stream discharge. Amplitude ranges from 0.17 m to 0.53 m. The large discrepancy in simulated streamflow discharge would indicate that there could be an important component of interbasin flow in the watershed.

The rest of the scenarios (base case, low K, and less precipitation) streamflow variabilities are shorter and smaller in agreement with recharge rates. Streamflow with a low K shows most of its variability during high recharge rates as occurs from 2015 through 2018. Outflow peaks are greatest at the end of the snow melting season. Whereas the lower recharge simulation shows a regular behavior according to the reduced recharge rate. A flatter curve for the base case displays a slower response to changes in recharge.

These discharge results, which are much higher than field observations, feed the idea that interbasin flow is an important component on the catchment.

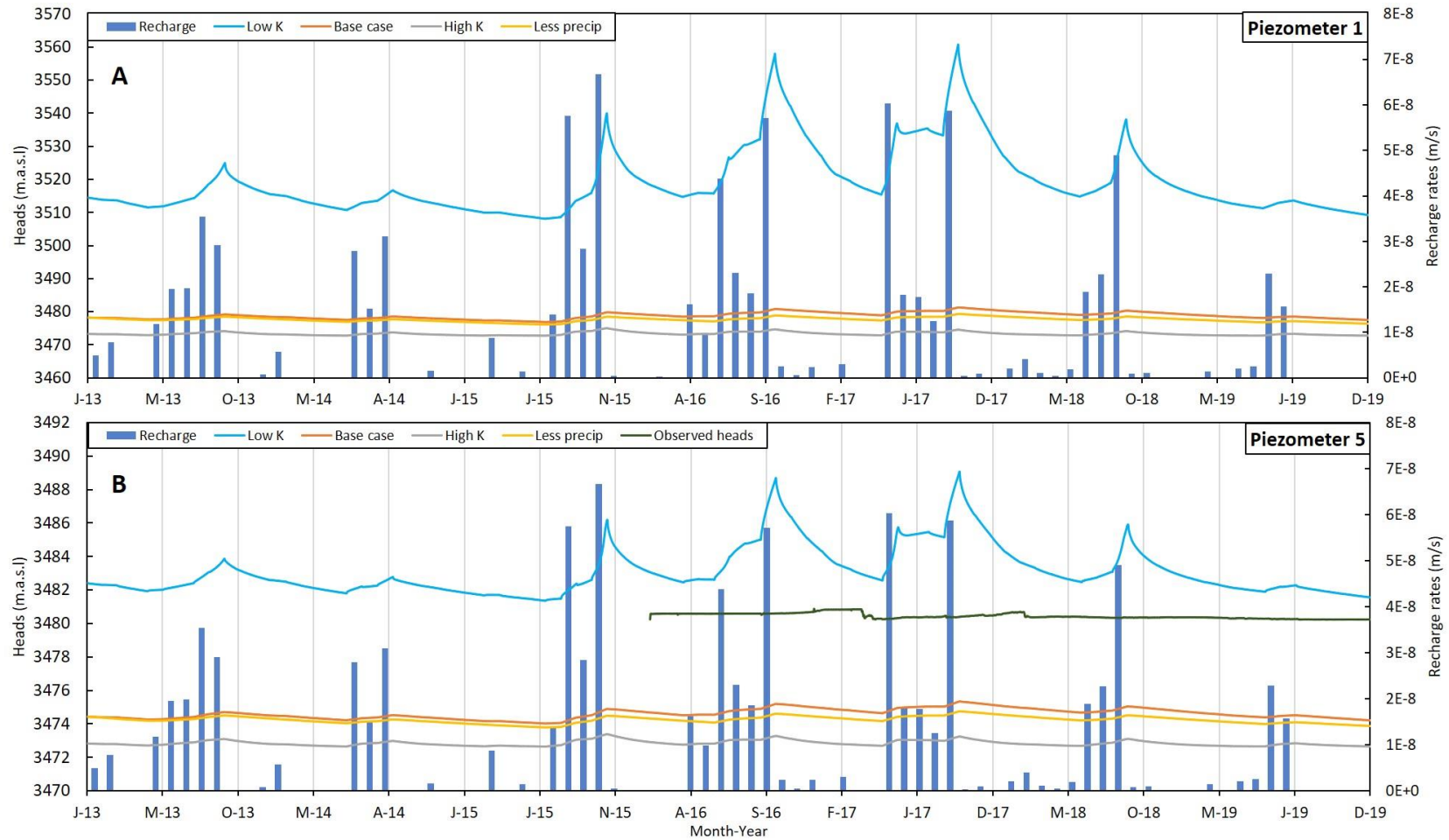


Figure 4.13: Simulated heads for the transient period A: Piezometer 1, next to Altar rock glacier. B: Piezometer 5 at the outlet of Altar watershed. Recharge rates are shown as bars.

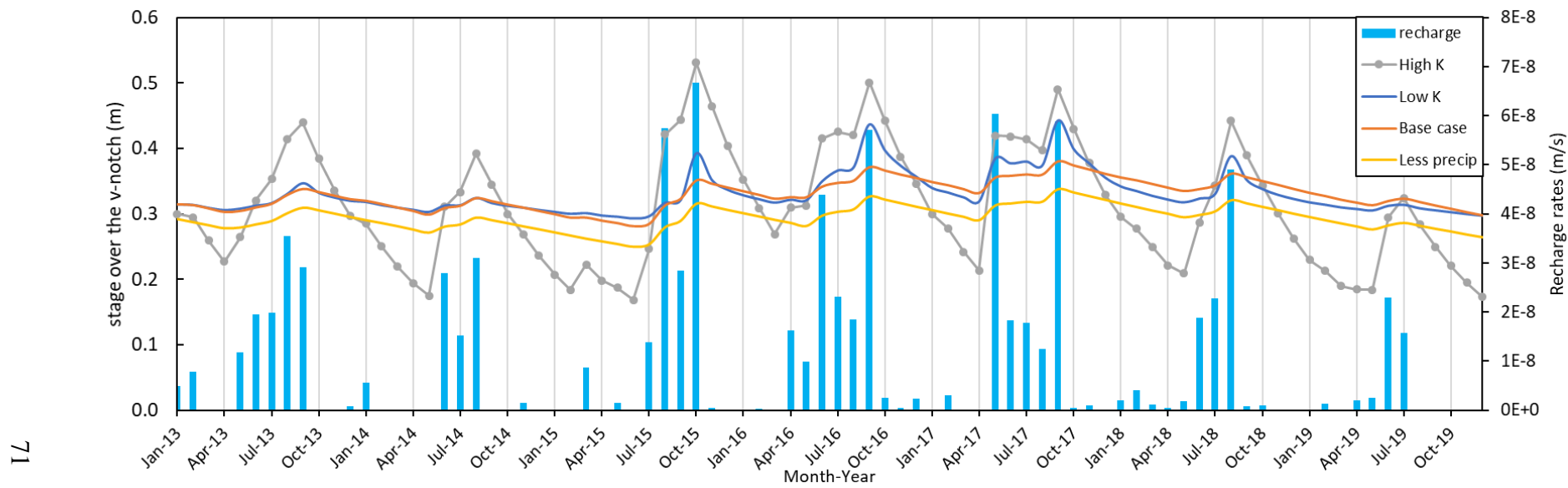


Figure 4.14: Stream discharge for the four scenarios.

4.8.3 Age distribution on groundwater

Age distributions were calculated for all scenarios using backward particle tracking from well P5 and the river cells in order to estimate travel times and distributions and to gain insight into the nature of the groundwater flow system. Mean and standard deviation of age for both analyses are shown in tables 6 and 7.

A total number of 175 particles are tracked backward from the location of the P5 well screen (15 m) to the water table. Well travel times are the highest when comparing both scenarios, meaning that particles take a longer time to travel from the location of the water table towards the well. Within this case, the base case scenario has the smallest estimated age and std dev with 143 yr and 14.9 respectively. The low K has the highest estimates with an average travel time of 184.6 yr whereas a high K case is between the two previous cases. Travel times are overall large if we think that particles have to overcome subsurface media and Ks distribution, flowing deep and laterally in the system before moving upward toward the well.

The river analysis has a total of 729 particles that have been tracked backward as well. Travel times are smaller than the well case which is feasible since surplus from groundwater will discharge on the drain and move out of the watershed with shorter travel times. In this case, a high K scenario provides the fastest travel estimates with a mean and std dev of 31 and 59.2 yr, respectively. Longer travel times come with a low K with a mean time of 83.3 yr whereas the base case is positioned in the middle of both cases. For all these three cases standard deviation values are large, representing that times vary amply within particles.

		Base case	Low K	High K
P5 Well particles	Mean travel times (yr)	143	184	154
	Std Dev (yr)	2	25	17
River particles	Mean travel times (yr)	45	83	31
	Std Dev (yr)	71	159	59

Table 4.2: Backward particle tracking from P5 well and river cells. Mean travel times and standard deviation are given in years.

Chapter 5

CONCLUSIONS AND OUTCOMES

5.1 Conclusions

The results above demonstrate the important link that exists in the Andes between snow accumulation and hydraulic heads. Groundwater discharge is affected by conditions such as temperature, elevation, angle of exposure, solar radiation, and season. Heads increase significantly with the spring season (after September) which is correlated with warmer temperatures and the first melting of the snowpack. The end of the melting season contributes with the largest discharge values in the study area. Similar patterns are also observable in other important rivers in the Province, where the biggest discharge events occur during the thawing spring. The decreases in hydraulic head take place around early-mid summer when all the snow has melted and the area gets back to its bare surface of gravel and loose rock. By then, the snowpack has melted and disappeared from the ground surface, at which time the glacier melting and groundwater continue to contribute to surface water discharge. The seasonal cycle restarts again once the first snowfalls happen around May-June and the system begins to accumulate snow for the next melting season. This pattern, although not observed in all wells, is considered to be the general pattern in the study area. On the other hand, stream discharges seem to be controlled primarily by groundwater availability.

In most cases the temperature records showed a seasonal behavior which corresponds to the conditions in those months. Slightly higher temperatures occurred during the spring and summer months, with a temperature decrease after March as the

winter season advance. A longer continuous data collection will help to further elucidate such behavior.

In addition to analysis of available data, the goal of assessing groundwater behavior and sensitivity analyses with ModelMuse was reached. Simulations predicted groundwater levels across the Altar watershed, however the prediction accuracy needs further examination. For this aim, we used available climate and borehole data, and certain assumptions to create a base-case scenario that approximates the Altar watershed. We then assess the system through sensitivity analysis to investigate its response to 3 different scenarios.

Hydraulic head observations at two piezometers were compared against simulations. Strong seasonality is only observed on the piezometer next to the rock glacier (P1) which shows a substantial response to melting which could indicate an important rock glacier input during the spring-half summer. The piezometer at the outlet of the watershed (P5) shows certain behaviors that are not completely understood adding some uncertainties, although since March 2018 holds a steadier trend.

Overall, results from simulations have not shown accurate correspondence with field data. A primary issue is uncertainty in the quality of the elevation data, both the DEM and the elevation surveys of wells and weirs. Degradation of weir structure was also a major problem. Lack of watershed-specific weather data, snow density estimates, lack of distribution and quality of hydrologic data were some field limitations that have added uncertainties to model outputs.

Simulated heads responses vary according to the K scenarios. Overall, simulations underestimate heads (except low K at P5) and overestimate discharges

according to field records. Differences may be an indication that the model is not adequately simulating a system, but it can also be attributed to different factors such as the DEM representativeness of steep terrains, survey errors, or data quality. Thus, better surveys are required to be able to use field data for model calibration.

Heads are quite variable in response to changes in recharge in a low-K scenario and they are marked by seasonality. On the other hand, the base case scenario, high-K, and less precipitation show smaller signals and steadier head responses compared to a low-K scenario. However, topography and K distribution play an important role.

Simulated stream discharge is much greater than observed in the field. Model simulated streamflow rates are more than 15x larger than field measurements. High streamflow rates are simulated for the base-case scenario and during the sensitivity analysis. Low-K and base case simulations show smaller variability than high-K simulations, whereas the low-recharge case has a lower discharge rate (by the amount of recharge reduction). The small response to changes in recharge is understandable since recharge is only varied by 15% in the low-recharge scenario, whereas K is varied by a factor of 10, and K/R is a controlling parameter. The large discrepancy in simulated streamflow compared to measured rates leads to think the conclusion that interbasin flow is an important factor in the Altar watershed.

Results from geochemical data show that the Altar area has local water recharge and tritium analyses of water from two monitoring wells showed < 0.2 TU. This indicates longer-term (>65 years) groundwater residence time. However, SF_6 analyses for these same two wells indicated shorter-term groundwater residence times (~ 10 -25 years), but these data may have been compromised by excess air contamination during sampling turning results seem younger. Results from

simulations with Modpath would support the tritium estimates. Simulated travel times for well particles suggest times at least of 143 yr.

This study has presented a broad insight into Andean watersheds and the hydrologic system in the area. Its location and focus have been unique for a groundwater approach in the Argentinean Andes. It is worth mentioning that the climatological dataset used has been unique for its record and location.

A continuation of research on the hydrology of alpine environment is encouraged, especially in semi-arid regions where the water resource is scarce and agricultural, industrial and hydropower activities heavily rely on discharges from Andean catchments. After all, any change to the hydrology system upstream in the Andes could subsequently have an effect downstream.

5.2 Uncertainties in model performance

5.2.1 Use of a DEM and elevation differences.

Digital elevation models (DEMs) have converted nowadays in an element product for earth sciences research. Their availability and free access on the Internet, their versatility in numerous fields such as modelling, geomorphology, or ecology among others, and the ease to get images from anywhere around the world have become them in an element tool in any research (Szypuła, 2019). Despite the wide coverage, they lack of detail either horizontal and vertical plays a factor. In areas of remote locations such as the Andes where the landscape is dominated by abrupt changes in elevation and steep slopes, DEMs are the best tools so far to obtain topographic maps. Elevation differences between observed heads and stream elevation

versus those simulated are between 5 meters. Considering the remote location and terrain, it could be considered a reasonable elevation error.

5.2.2 Recharge parameters and snow density estimate.

Some uncertainty with the weather data can be arguable. Precipitation is measured with a tipping bucket, but in sites over 3500 m.a.s.l. conditions are variable and constantly changing which may make the device to not work properly. As it is mentioned by Colli, et al. (2014), under frozen precipitation or heavy rainfall the tipping bucket rain gauge may not operate well. Another potential error source could come when rain is driven by strong winds, which can impact the accuracy of measurements. On the other hand, the snowmelt factor computed to convert snow height to snowmelt was fixed throughout the seasons. Although this is not what in reality happens, it demonstrated a good overlap between field data and Pelambres data set, which hold that if there was a discrepancy, would not be a big magnitude. These small fixes should expose and demonstrate the lack of crucial parameters, considering the importance that the snowpack from previous season plays in the region. Accords between mining company and water government offices should be encourage to get better and detailed weather data at high elevation in the Andes.

5.2.3 Subsurface layout

Little is known about the Altar subsurface domain. Mining boreholes do exist but they focus on ore content only, rather than hydrologic characteristics. No records of stratigraphy or geophysics were found. Pump tests were planned out, but once in the field were not feasible to carry out due to the state of the well. Observations on geophysics exist in the surrounding of Altar project and part of the Altar valley, but

unfortunately, they stop short and do not investigate the watershed itself. In order to understand Altar subsurface, borehole data was used. Rock quality design was used as a measure of hardness and core integrity. As of today, more than hundred ore drills exist, and in some cases reaching up 1000 m deep. A well detailed geophysics survey from top ridges to the bottom valley would help to define in a better way layers and shorten uncertainties.

5.3 Future work

The present work pioneers for groundwater modeling in this part of the Argentinean Andes and can potentially be used as a reference for future or similar research. There are several potential lines of research to pursue that are identified from this study. A major outcome is that interbasin flow should be considered an important component in Andean watershed, therefore exploring other boundary conditions such as a constant head at the outlet of the watershed, or expanding the domain boundary can give insights into this process.

The use of snow models to simulate mountain snowpack and melting processes could also substantially improve estimates of recharge rates and timing. Snow spatial distribution and temporal variability is highly important for Andean communities and in a wide range of environments. Several factors affect mountain snowpack that could be better understood with a snow-evolution model whose implementation could lower uncertainties in snow covered regions and model results.

There is great interest in the influence of the Altar rock glacier on the hydrologic system. Located on top of the watershed, two wells were drilled but unfortunately one went dry and the other has not recorded successfully a complete record. Conservative recharge estimates from the limited data obtained indicate that

the rock glacier recharge is locally significant, greater than 3-5x the estimated recharge rate over the rest of the watershed. The overall contribution to the watershed recharge is smaller but non-negligible, making up at least 10% of total recharge. Equipping the area with deeper wells and obtaining longer head records would help to improve estimates and understanding of rock glacier contribution into the system. This is critical not only for the overall water budget but also for the mining company, government, and communities downstream.

The implementation of a better and broad well network with continuous records would help to calibrate the model and lower uncertainties. Drilling in the Andes is not easy, the remote location coupled with the associated cost make it an important budget component. Three extra new wells up to 80 m deep were drilled since 2019 however, they went dry. Future work should aim to expand groundwater data and get accurate weather parameters.

It is clear that gaining insight into mountain regions would benefit several actors and provide knowledge into Andean watersheds. This would greatly contribute to society by improving water management and supply downstream, as well as being able to predict water risks in the future. Scientific research on these aspects could help to understand what the future might hold for those dependent on water supplies in arid and semi-arid regions.

REFERENCES

- Albrecht, R. (2012). Groundwater Modelling in the Andes: Balancing Industry and Environment. Van Walt.
(<https://www.vanwalt.com/news/2012/11/20/groundwater-modelling-in-the-andes-balancing-industry-and-environment/>).
- Alford, D. (1985), Mountain hydrologic systems, Mountain Research and Development 5, 349–393, doi:10.2307/3673296.
- Ansilta S.R.L. (2010). Informe hidrogeologico ambiental a base de geologia de campo, geofisica y antecedentes recibidos del comitente.
- Bales, R. C., N. P. Molotch, T. H. Painter, M. D. Dettinger, R. Rice, and J. Dozier (2006). Mountain hydrology of the western United States. Water Resour. Res., 42, W08432.
- Baraer, M., McKenzie, J., Mark, B., Gordon, R., Bury, J., Condom, T., Gomez, J., Knox, S., Fortner, S. (2015). Contribution of groundwater to the outflow from ungauged glacierized catchments: a multi-site study in the tropical Cordillera Blanca, Peru. Hydrological Processes 29, 2561-2581.
- Baraer, M., McKenzie, J.M., Mark, B.G., Burt, J., Knox, S. (2009). Characterizing contributions of glacier melt and groundwater during the dry season in a poorly gauged catchment of the Cordillera Blanca (Peru). Adv. Geosci., 22, 41-49.
- Barnett, T. P., Adam, J. C., and Lettenmaier, D. P. (2005). Potential impacts of a warming climate on water availability in snow-dominated regions, Nature, 438, 303–309.
- Blessent, D., Barco, J., Tranquille Temgoua, A.G., Echeverri-Ramirez, O. (2017). Coupled surface and subsurface flow modeling of natural hillslopes in the

- Aburra valley (Medellín, Colombia). *Hydrogeol Journal*, 25:331-345, doi 10.1007/s10040-016-1482-z.
- Bortels K., Gascoïn S., Kinnard C., Liston G., Lhermitte S. (2013). Wind effects on snow cover in Pascua-Lama, Dry Andes of Chile. *Advances in Water Resources* 55, 25-39.
- Bradley RS, Vuille M, Diaz HF, Vergara W (2006) Threats to water supplies in the tropical Andes. *Science* 312(5781):1755–1756.
<https://doi.org/10.1126/science.1128087>
- Bradley, R. S., Vuille, M., Diaz, H. F., and Vergara, W.: Threats to water supplies in the tropical Andes, *Science*, 312, 1755-1756, 2006.
- Bradley, R.S., Keimig, F.T., and Diaz, H.F. (2004). Projected temperature changes along the the American cordillera and the planned GCOS network. *Geophys. Res. Lett.*, 31, L16210, doi:10.1029.
- Bredehoeft J. D. (2005). The conceptualization model problem-surprise. *Hydrogeol. J.* 13:37-46.
- Briner, S., Elkin, C., Huber, R., Gret-Regamey, A. (2012). Assessing the impacts of economic and climate changes on land-use in mountain regions: A spatial dynamic modeling approach. *Agriculture, Ecosystems and Environment*, 149, 50-63.
- Citation: Nyende J, Van TG, Vermeulen D (2013) Conceptual and Numerical Model Development for Groundwater Resources Management in a Regolith-Fractured-Basement Aquifer System. *J Earth Sci Clim Change* 4: 156. doi:10.4172/2157-7617.1000156

- Clow DW, Schrott L, Webb R, Campbell DH, Torizzo A, Dornblaser M. 2003. Ground water occurrence and contributions to streamflow in an alpine catchment, colorado front range. *Ground Water* 41: 937–950
- de Jong C. (2015) Challenges for mountain hydrology in the third millennium. *Front. Environ. Sci.* 3:38. doi: 10.3389/fenvs.2015.00038
- Delbart, N., Dunesme, S., Lavie, E., Madelin, M., Goma, R. (2015). Remote sensing of Andean mountain snow cover to forecast water discharge of Cuyo rivers. *Journal of Alpine Research*, 130-2.
- Earth Explorer; 2000; FS; 083-00; Geological Survey (U.S.)
- Falvey M, Garreaud R (2007) Wintertime precipitation episodes in Central Chile: associated meteorological conditions and orographic influences. *J Hydrometeorol* 8:171–193
- FAO. Food and Agriculture Organization of the United Nations. Mountains as the water towers of the world. (www.fao.org)
- Fetter, C. W. 1. (1994). *Applied hydrogeology*. 3rd ed. New York : Toronto : New York: Macmillan.
- Forster, C. B., and Smith, L. (1988). Groundwater flow systems in mountainous terrain: 2, Controlling factors, *Water Resources Research* 24, 1011 – 1023.
- Gárfias, J. (NA). Groundwater in mountain regions. *Groundwater*. Vol. I. *Encyclopedia of Life Support Systems (EOLSS)*.
- Garreaud, R.D., et al., Present-day South American climate, *Paleogeogr. Palaeoclimatol. Palaeoecol.* (2008), doi: 10.1016/j.palaeo.2007.10.032
- Gebreyohannes, T., De Smedt, F., Walraevens, K., Gebresilassie, S., Hussien, A., Hagos, M., Amare, K., Deckers, J., Gebrehiwwot, K. (2017). Regional

- groundwater flow modeling of the Geba basin, northern Ethiopia. *Hydrogeological Journal* 25, 639- 655.
- Gerrard, J. (1990). *Mountain Environments: An Examination of the Physical Geography of Mountains*, The MIT Press, 317 pp. Cambridge, Mass.
- Gleeson, T., and Manning S. (2008). Regional groundwater flow in mountainous terrain: three- dimensional simulations of topographic and hydrogeologic controls. *Water Resources Research* 44, W10403, doi:10.1029/2008WR006848.
- Guzman, P., Anibas, C., Batelaan, O., Huysmans, M., Wyseure, G. (2016). Hydrological connectivity of alluvial Andean valleys: a groundwater/surface-water interaction case study in Ecuador. *Hydrogeological Journal* 24:955-969, doi 10.1007/s10040-015-1361-z.
- Haitjema, H. M., and S. Mitchell-Bruker (2005), Are water tables a subdued replica of the topography?, *Ground Water*, 43(6), 781–786, doi:10.1111/j.1745-6584.2005.
- Harbaugh, A.W. (2005). MODFLOW-2005, The U.S. Geological Survey modular ground-water model—the Ground-Water Flow Process: U.S. Geological Survey Techniques and Methods 6- A16, variously p.
- Harbaugh, A.W., Banta, E.R., Hill, M.C., McDonald, M.G. (2000). MODFLOW 2000. The US Geological Survey modular groundwater model-user guide to modularization concepts and the groundwater flow process. US Geol Surv Open-File.
- Hayashi, M. (2019). *Alpine Hydrogeology: The critical role of groundwater in sourcing the headwaters of the World*. National Ground Water Association. Doi: 10.1111/gwat.12965

Henderson, F.M. Open Channel Flow, 1st ed.; Prentice–Hall: Upper Saddle River, NJ, USA, 1966; ISBN 9780-0235-3510-9

Hood JL, Roy JW, Hayashi M. 2006. Importance of groundwater in the water balance of an alpine headwater lake. *Geophysical Research Letters* 33. DOI: 10.1029/2006GL026611

Huntington J.L., and Niswonger R.G. (2012). Role of surface-water and groundwater interactions on projected summertime streamflow in snow dominated regions: An integrated modeling approach. *Water Resources Research*, 48, W11524.

Informe Mantención estaciones meteorológicas Minera Peregrine. Ingeniería y Proyectos Ltda. 2019.

Intergovernmental Panel on Climate Change (2001), *Climate Change 2001: Impacts, Adaptation, and Vulnerability: Contribution of Working Group II to the Third Assessment Report of the Intergovernmental Panel on Climate Change*, edited by J. J. McCarthy et al., Cambridge Univ. Press, New York.

Jódar, J., Cabrera, J.A., Martos-Rosillo, S., Ruiz-Constan, A., Gonzalez-Ramon, A., Lamban, L.J., Herrera, C., Custodio, E. (2017). Groundwater discharge in high-mountain watersheds; A valuable resource for downstream semi-arid zones. The case of the Berchules River in Sierra Nevada (Southern Spain). *Science of the Total Environment* 593-594, 760-772.

John Shen (1981). Discharge characteristics of triangular-notch thin-plate weirs. Geological Survey water-supply paper 1617-B.

Kao, Y-H., Liu, C-W., Wang, S-W., Lee, C-H. (2012). Estimating mountain block recharge to downstream alluvial aquifers from standard methods. *Journal of Hydrology* 426-427, 93-102.

- Katsuyama, M., N. Ohte, and N. Kabeya (2005), Effects of bedrock permeability on hillslope and riparian groundwater dynamics in a weathered granite catchment. *Water Resour. Res.* 41, W01010, doi:10.1029/2004WR003275.
- Kernodle, J. M.; McAda, D. P.; Thorn, C. R. (1995). Simulation of ground-water flow in the Albuquerque basin, central New Mexico, 1901-1994, with projections to 2020. U.S Geological Survey. Water- Resources Investigations report 94-4251
- Kinoti, Irene K. (2018). Integrated hydrological modeling of surface and groundwater interactions in Heuningnes catchment (South Africa). Thesis
- Kundzewicz, Z. W., Mata, L. J., Arnell, N. W., Döll, P., Jimenez, B., Miller, K., Oki, T., Sen, Z. & Shiklomanov, I. (2008) The implications of projected climate change for freshwater resources
- Manning, A. H., and Solomon, D. K. (2005). An integrated environmental tracer approach to characterizing groundwater circulation in a mountain block. *Water Resources Research* 41, W12412, doi:10.1029/2005WR004178.
- Masiokas, M.H., Villalba, R., Luckman, B.H., Le Quesne, C., Aravena, J.C. (2006). Snowpack variations in the central Andes of Argentina and Chile, 1951-2005: large-scale atmospheric influences and implications for water resources in the region. *American Meteorological Society. Journal of climate.* Vol.19.
- Mata, L. J. & Campos, M. (2001) Latin America. In: *Climate Change 2001: Impacts, Adaptation, and Vulnerability. Contribution of Working Group II to the Third Assessment Report of the Intergovernmental Panel on Climate Change* (ed. by J. J. McCarthy, O. F. Canziani, N. A. Leary, D. J. Dokken & K. S. White), 693–734. Cambridge University Press, Cambridge, UK

- Mata, L. J. & Campos, M. (2001) Latin America. In: Climate Change 2001: Impacts, Adaptation, and Vulnerability. Contribution of Working Group II to the Third Assessment Report of the Intergovernmental Panel on Climate Change (ed. by J. J. McCarthy, O. F. Canziani, N. A. Leary, D. J. Dokken & K. S. White), 693–734. Cambridge University Press, Cambridge, UK
- McDonald, M.G., and Harbaugh, A.W. (1988). A modular three-dimensional finite-difference ground-water flow model: U.S. Geological Survey Techniques of Water-Resources Investigations,
- Mernild, S. H., Liston, G. E., Hiemstra, C. A., Malmros, J. K., Yde J. C., and McPhee, J. (2017). The Andes Cordillera. Part I: snow distribution, properties, and trends (1979-2014), *Int. J. Climatol.*, 37, 1680-1698.
- Meybeck, M., P. Green, and C. Vorosmarty (2001). A new typology for mountains and other relief classes, *Mountain Research and Development* 21, 34 – 45, doi:10.1659/0276-741.
- Montecinos A, Aceituno P. Seasonality of the ENSO-related rainfall variability in the Central Chile and associated circulation anomalies. *JClimate*. 2003;16(2):281-296.
- Morris, D.A. and A.I. Johnson, 1967. Summary of hydrologic and physical properties of rock and soil materials as analyzed by the Hydrologic Laboratory of the U.S. Geological Survey, U.S. Geological Survey Water-Supply Paper 1839-D, 42p.
- Mountain Pass Consulting, 2012.; Resultado de Actividades de Monitoreo, y Caracterización de Geoformas Glaciales y Peri-Glaciales. Valle del Altar, San Juan, Argentina.

- Mountain Pass Consulting, 2013.; Resultado de Actividades de Monitoreo, y
 Caracterización de Geoformas Glaciales y Peri-Glaciales. Valle del Altar, San
 Juan, Argentina.
- Mountain Pass Consulting, 2014.; Resultado de Actividades de Monitoreo, y
 Caracterización de Geoformas Glaciales y Peri-Glaciales. Valle del Altar, San
 Juan, Argentina.
- Mountain Pass Consulting, 2015.; Resultado de Actividades de Monitoreo, y
 Caracterización de Geoformas Glaciales y Peri-Glaciales. Valle del Altar, San
 Juan, Argentina.
- Mulligan, M., Rubiano, J., Hyman, G., White, D., Garcia, J., Saravia, M., Leon, J.G.,
 Selvaraj, J., Gutierrez, T., Saenz-Cruz, L.L. (2012). The Andes basins:
 biophysical and developmental diversity in a climate of change. *Water
 International*. Vol. 35, No. 5, 472-492.
- Neilsen, D., G. Duke, B. Taylor, J. Byrne, S. Kienzle, and T. Van der Gulik (2010),
 Development and verification of daily gridded climate surfaces in the Okanagan
 Basin of British Columbia, *Can. Water Resour. J.*, 35(2), 131–154
- Novoa, J. E. & López, D. (2001) IV Región: El Escenario Geográfico Físico. In: Libro
 Rojo de la Flora Nativa de la Región de Coquimbo y de los Sitios Prioritarios
 para su Conservación (ed. by F. A. Squeo, G. Arancio & J. R. Gutiérrez), 13–
 28. Ediciones de la Universidad de La Serena, La Serena, Chile.
- Ossa-Moreno, J., Keir, G., McIntyre, N., Cameletti, M., Rivera, D. (2019). Comparison
 of approaches to interpolating climate observations in steep terrain with low-
 density gauging networks. *Hydrol. Earth Syst. Sci.*, 23, 4763-4781.
- Paterson, W. S. B. (1994). *The Physics of Glaciers*. Third edition.

- Pepin, N., Bradley, R.S., Díaz, H.F., Baraer, M., Caceres, E.B., Forsythe, N., Fowler, H., Greenwood, G., Hashmi, M.Z., Liu, X.D. (2015). Elevation-dependant warming in mountain regions of the world. *Nat. Clim. Change* 5, 424-430.
- Phillips, F. M., Castro, M. C. (2003). *Groundwater Dating and Residence time Measurements*. University of Michigan, Ann Arbor, USA.
- Ruelland, D., Brisset, N., Jourde, H., Oyarzun, R. (2011). Modeling the impact of climatic variability on groundwater and surface flows from a mountainous catchment in the Chilean Andes. *Cold region hydrology in a changing climate*, IAHS Publ. 346.
- Scanlon, B. R., K. E. Keese, A. L. Flint, L. E. Flint, C. B. Gaye, W. M. Edmunds, and I. Simmers (2006), Global synthesis of groundwater recharge in semiarid and arid regions. *Hydrogeol. J.*, 20, 3335–3370, doi:10.1002/hyp.6335.
- Shumlich, A. (2018). *Measuring the topography and motion of rock glaciers in the Cordillera Principal, Argentina*. Unpubl. Master's Thesis, University of Delaware.
- Schrott, L.: The hydrological significance of high mountain permafrost and its relation to solar radiation, A case study in the high Andes of San Juan, Argentina. *Bamberger Geographische Schriften*, Bd, 15, 71-84, 1998.
- Smerdon, B.D., Allen, D.M., Grasby, S.E., Berg, M.A. (2009). An approach for predicting groundwater recharge in mountainous watersheds. *Journal of Hydrology* 365, 156-172.
- Somers, L. D., McKenzie, J. M., Mark, B. G., Lagos, P., Ng, G.-H. C., Wickert, A. D., et al. (2019). Groundwater buffers decreasing glacier melt in an Andean watershed-but not forever. *Geophysical Research Letters*, 46.

- Somers, L., Gordin, R., McKenzie, J.M., Lautz, L.K, Wigmore, O., Glose, A, Glas, R., Aubry-Wake, C., Mark, B., Baraer, M., Condom, T. (2016). Quantifying groundwater-surface water interactions in a proglacial valley, Cordillera Blanca, Peru. *Hydrol. Process.* 30, 2915-2929.
- Staudinger, M., Stoelzle, M., Seeger, S., Seibert, J., Weiler, M., Stahl, K. (2017). Catchment water storage variation with elevation. *Hydrol. Process.* 1099-1085. 10.1002/hyp. 11158.
- Teotop, 2011. Algunas consideraciones orientativas preliminares sobre cuantificación y sustentabilidad del agua subterránea Proyecto Altar.
- Tromp-van Meerveld, H. J., Peters, N.E., McDonnell, J.J., (2007). Effect of bedrock permeability on subsurface stormflow and the water balance of a trenched hillslope at the Panola Mountain Research Watershed, Georgia, USA. *Hydrol. Process.* 21, 750.769.
- U.S. Geological Survey, (2020). The reston Groundwater Dating Laboratory, Dating with SF6 background, accessed January 25, 2021 at URL <https://water.usgs.gov/lab/sf6/background/>
- Uchida, T., Y. Asano, N. Ohte, and T. Mizuyama (2003), Seepage area and rate of bedrock groundwater discharge at a granitic unchanneled hill-slope. *Water Resour. Res.*,39(1), 1018, doi:10.1029/2002WR001298.
- Urrutia, J., Jódar, J., Medina, A., Herrera, C., Chong, G., Urqueta, H., Luque, J. (2018). Hydrology and sustainable future groundwater abstraction from the Agua Verde aquifer in the Atacama Desert, northern Chile. *Journal of Hydrology* 26;1989-2007.

- Vector Argentina S.A., 2008.; Estudio de Línea de Base Estudio Hidrogeológico. Etapa II. Proyecto Altar, San Juan. Argentina.
- Vector Argentina S.A., 2008.; Estudio de Línea de Base Estudio Hidrogeológico. Etapa I. Proyecto Altar, San Juan. Argentina.
- Viale, M. and Garreaud, R. (2015). Orographic effects of the subtropical and extratropical Andes on upwind precipitating clouds. *J. Geophys. Res.-Atmos.*, 120, 4962-4974.
- Viale, M. and Nuñez, M. N. (2011). Climatology of winter orographic precipitation over the subtropical central Andes and associated synoptic and regional characteristics. *J. Hydrometeorol.*, 12, 481-507.
- Vicuña, S., Garreaud, R., and McPhee, J.: Climate change impacts on the hydrology of a snowmelt driven basin in semiarid Chile, *Climatic Change*, 105, 469–488, 2011.
- Viviroli, D., and Weingartner, R. (2004). The hydrological significance of mountains: From regional to global scale. *Hydrology & Earth System Sciences* 8,1016–1029.
- Viviroli, D., M. Kummu, M. Meybeck, and Y. Wada. 2019. Increasing dependence of lowland population on mountain water resources. *EarthArXiv*.
<https://doi.org/10.31223/osf.io/fr5u>
- Voekler, H.M., Allen, D.M., Alila, Y. (2014). Modeling coupled surface water – Groundwater processes in a small mountainous headwater catchment. *Journal of Hydrology* 517, 1089-1106.
- Wahl, K. L., 1992: Evaluation of trends in runoff in the western United States. *Managing Water Resources during Global WARMING* 2006 LISTON AND

ELDER 1275 Change, R. Herrmann, Ed., American Water Resources Association, 701–710.

- Welch, L. A., Allen, D.M., and Van Meerveld H.J. (2012), Topography controls on deep groundwater contributions to mountain headwater streams and sensitivity to available recharge. *Canadian Water Resources Journal/Revue canadienne des ressources hydriques*, 37:4, 349-371, doi:10.4296.
- Welch, L. A., and Allen, D.M., (2012), Consistency of groundwater flow patterns in mountainous topography: Implications for valley bottom water replenishment and for defining groundwater flow boundaries. *Water Resour. Res.*, 48, W05526, doi:10.1029.
- Williams MW, Knauf M, Caine N, Liu F, Verplanck PL. 2006. Geochemistry and source waters of rock glacier outflow, Colorado Front Range. *Permafrost and Periglacial Processes* 17:13–33.
- Wilson, J. L., and Guan, H. (2004). Mountain-block hydrology and mountain-front Recharge. *Groundwater Recharge in a Desert Environment: The Southwestern United States*, pp. 113–137, AGU, Washington, D. C.
- Winston, Richard B. (2009). *ModelMuse : a graphical user interface for MODFLOW-2005 and PHAST*. Reston, Va. :U.S. Geological Survey,
- Wohl, E. (2000). *Mountain Rivers*. Water Resource. Monograph 14 320 pp., Washington, D. C.
- Zambrano-Bigiarini, M., Nauditt, A., Birkel, C., Verbist, K., and Ribbe, L. (2016). Temporal and spatial evaluation of satellite-based rainfall estimates across the complex topographical and climatic gradients of Chile, *Hydrol. Earth Syst. Sci.*, 21, 1295-1320.

Appendix A

SUPPLEMENTAL MATERIAL

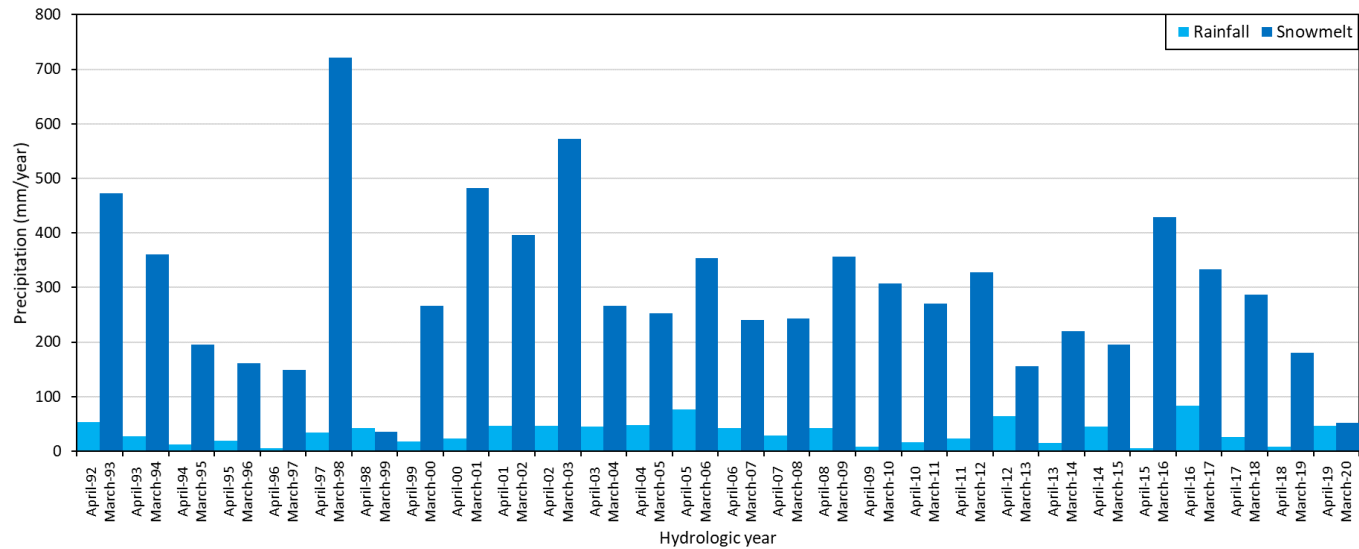


Figure Apx 10: Precipitation from Pelambres Mining (Chile), according to the hydrologic year (April-March since 1992-2020).
Source: Pelambres Mining

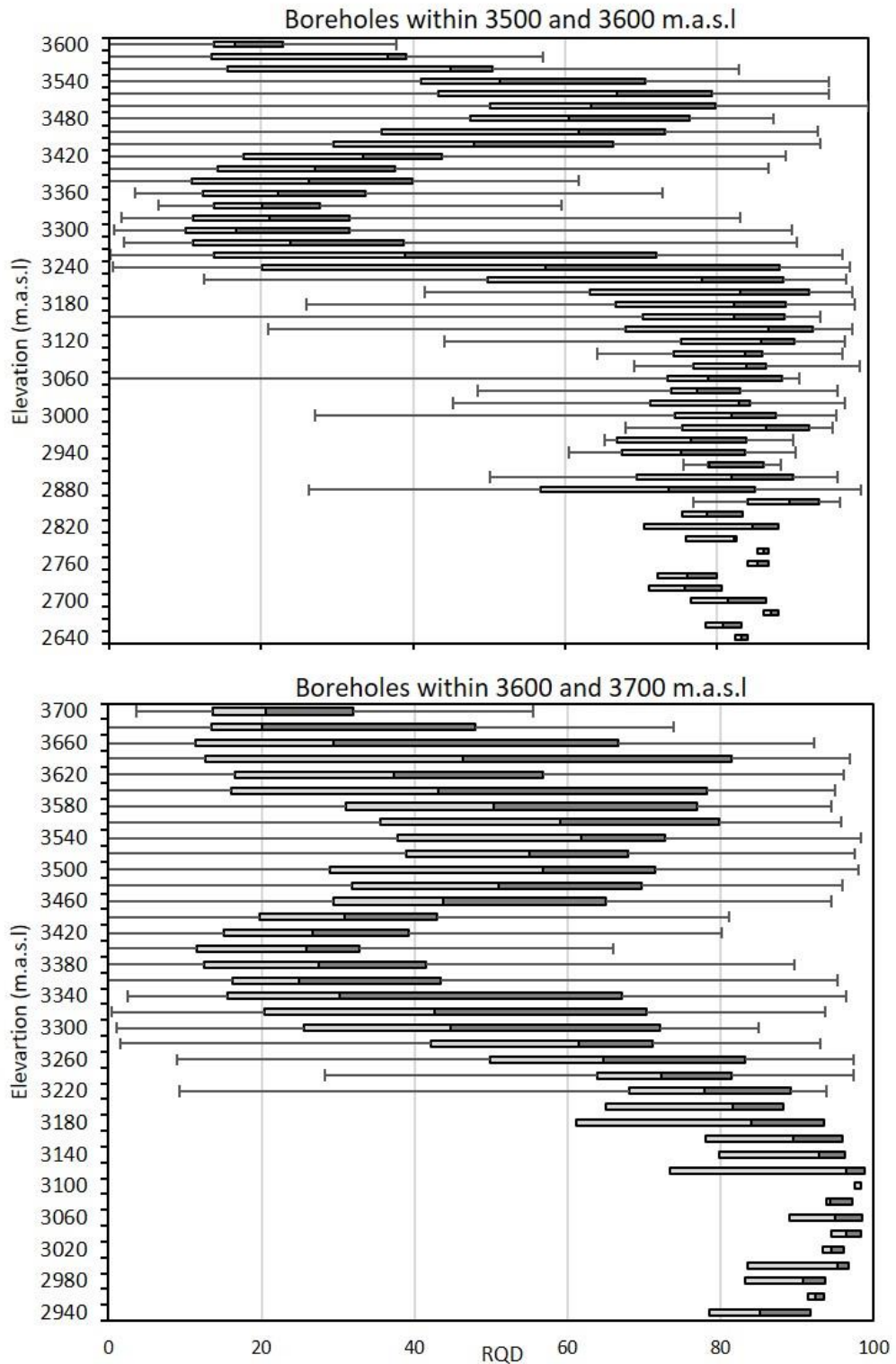


Figure Apx 11: Borehole data from Altar site according to elevation bands and RQD (rock quality design)

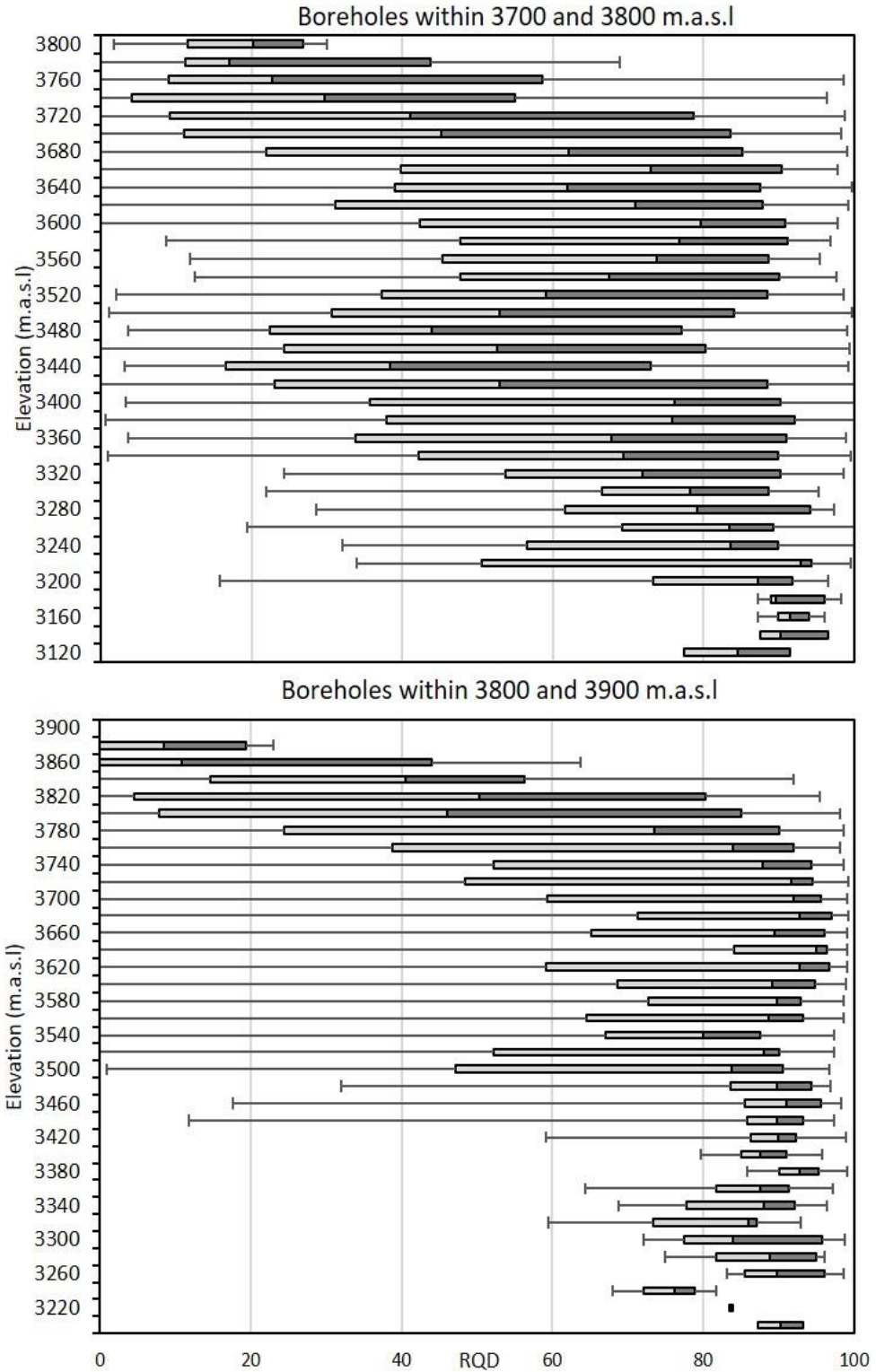


Figure Apx 12: Borehole data from Altar site according to elevation bands and RQD (rock quality design)

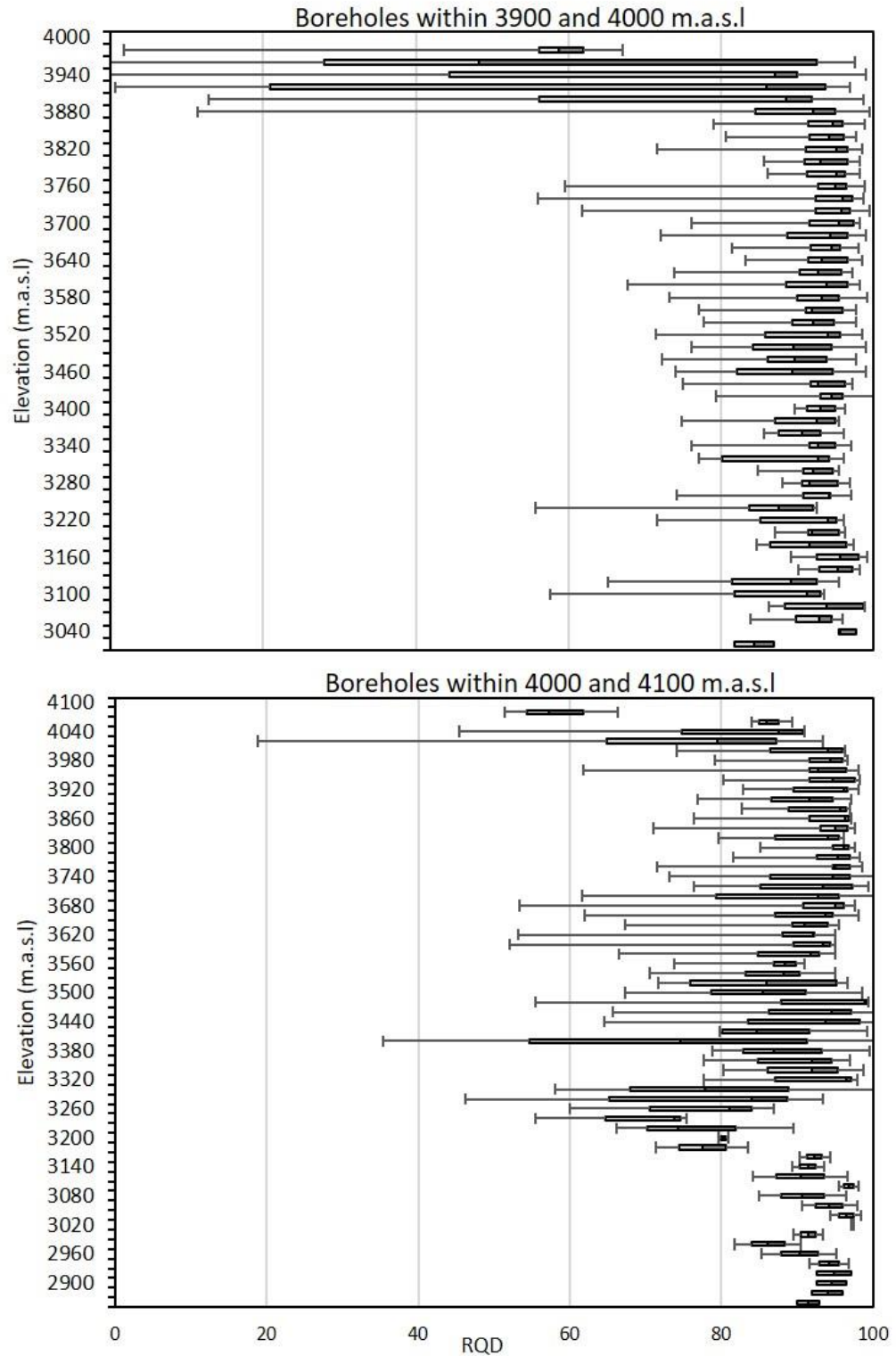
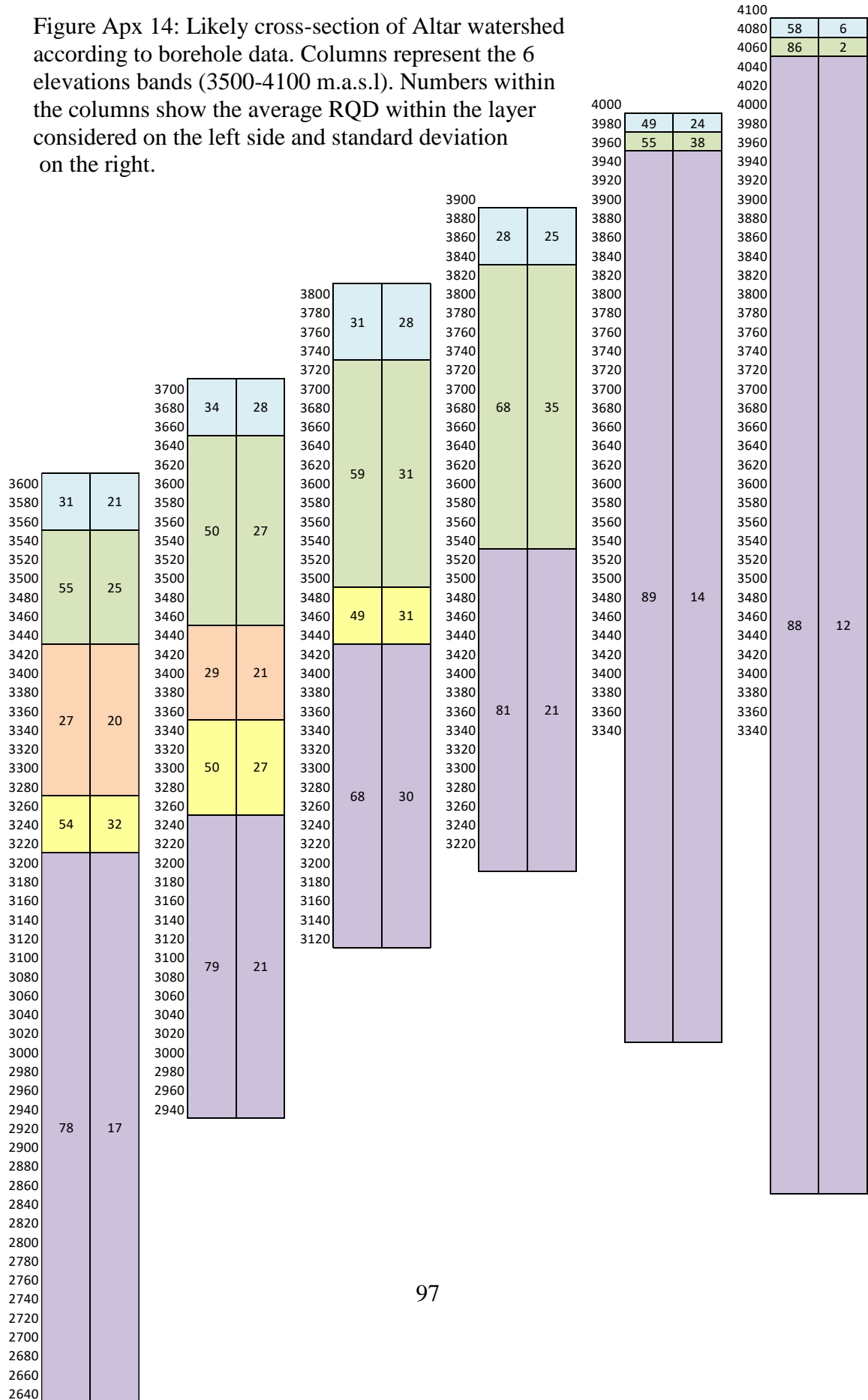


Figure Apx 13: Borehole data from Altar site according to elevation bands and RQD (rock quality design)

Figure Apx 14: Likely cross-section of Altar watershed according to borehole data. Columns represent the 6 elevations bands (3500-4100 m.a.s.l.). Numbers within the columns show the average RQD within the layer considered on the left side and standard deviation on the right.



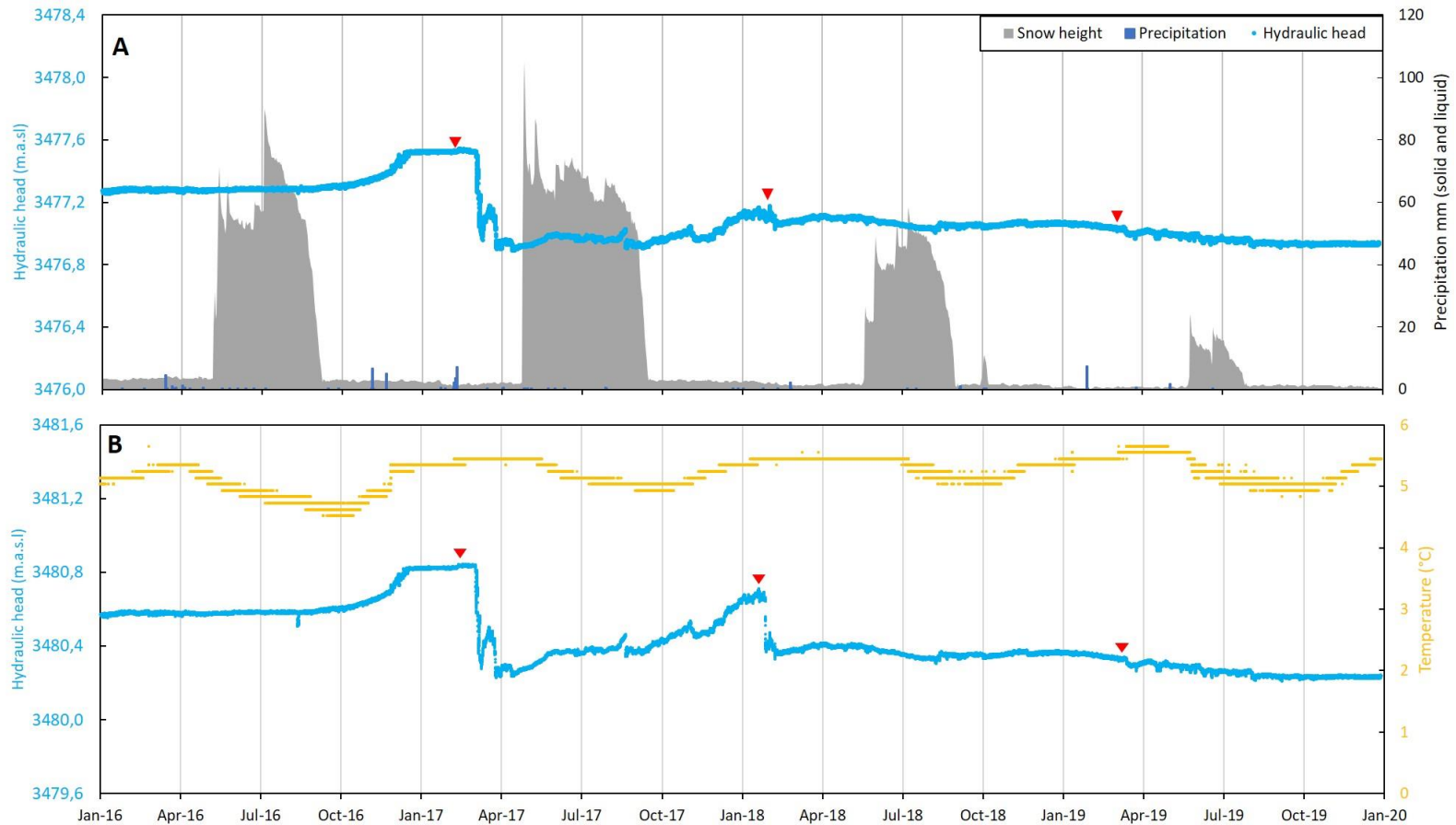


Figure Apx 15: A: Water table and precipitation for piezometer P5. Heads are according to DEM elevation pixel at the well (3477.08 m.a.s.l.). Well casing: 0.45 m. B: Water table elevation and temperature for piezometer P5. Time-lapse 2016-2020. Alt. 3480.4 m.a.s.l.

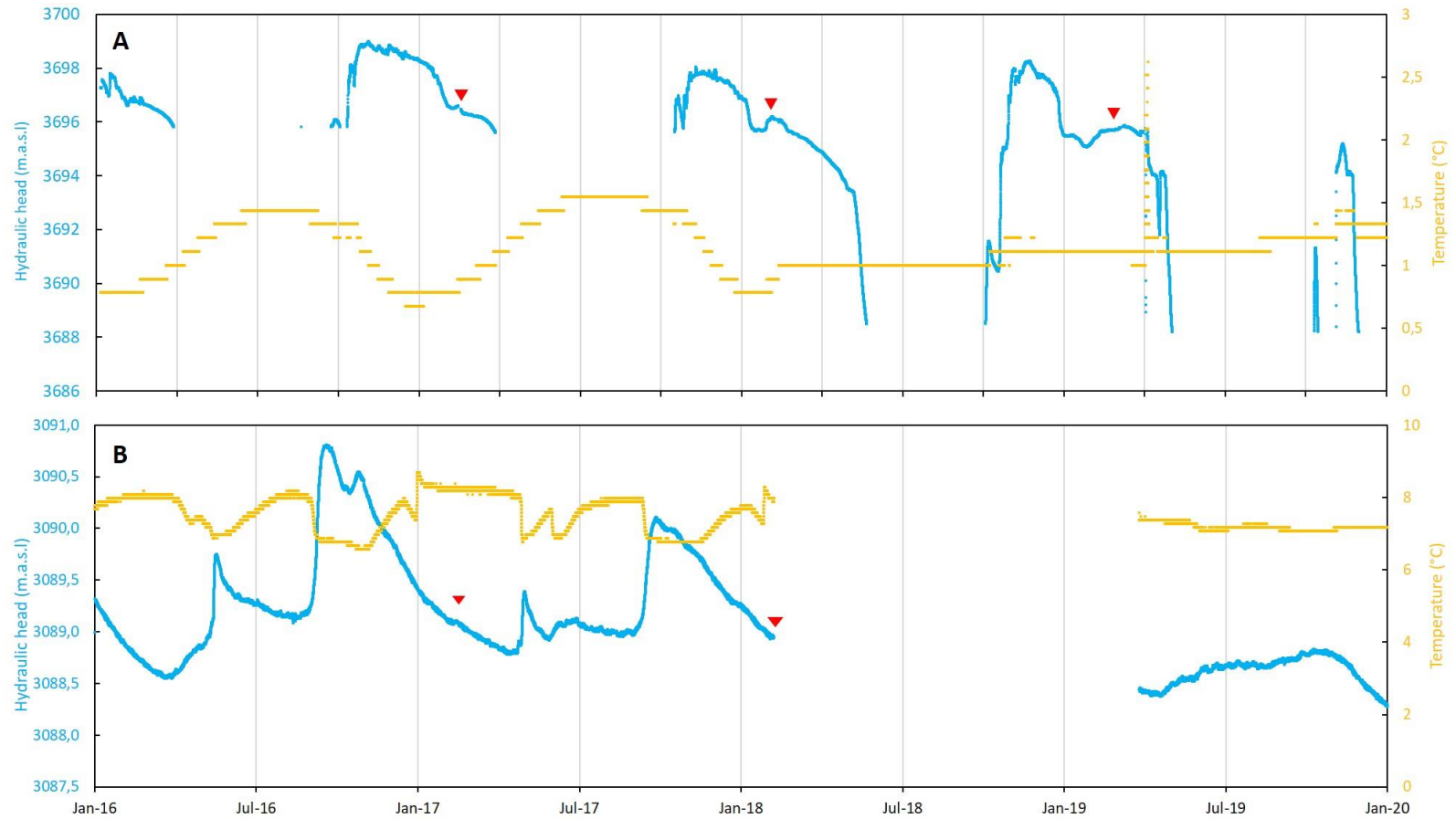


Figure Apx 16: A: Water table elevation and temperature for P1 next to a rock glacier. Alt. 3705 m a.s.l. B: Same that above for piezometer P6. Alt. 3105 m.a.s.l. Red triangles indicate data logger removal and the start of a new data long-term deployment. Gaps in data indicate lacks of measurements.

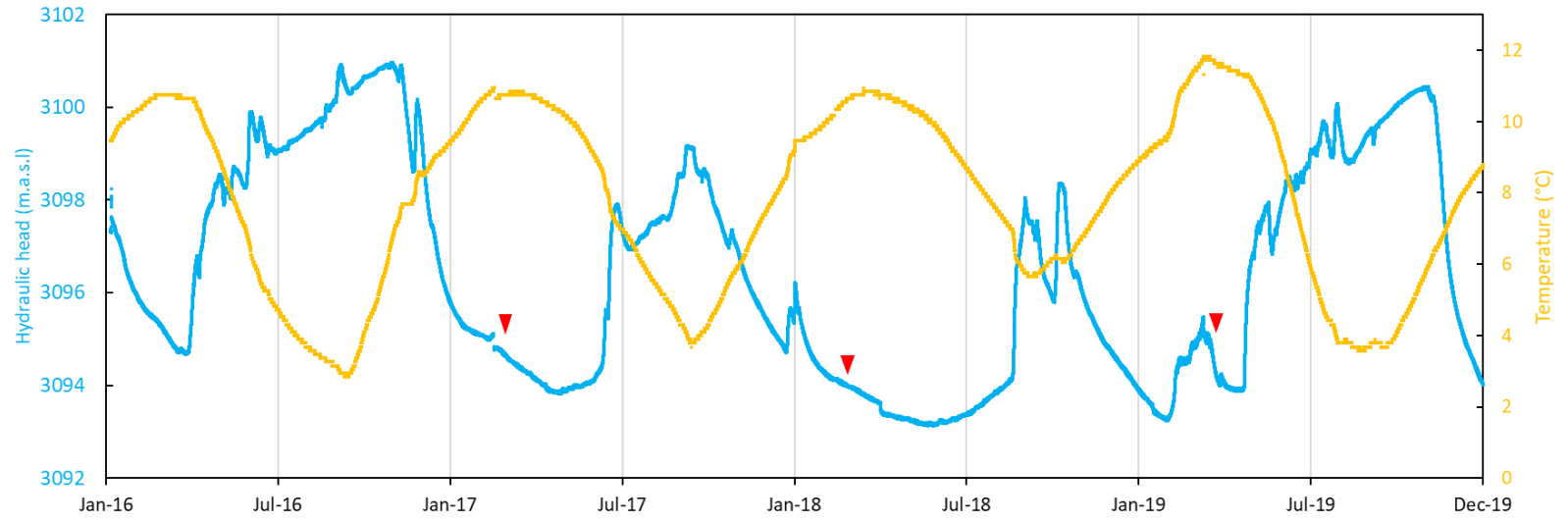


Figure Apx 17: Water table and temperature for piezometer P7. Alt. 3103 m.a.s.l. Red triangle indicates data logger removal and the start of a new data long-term deployment.

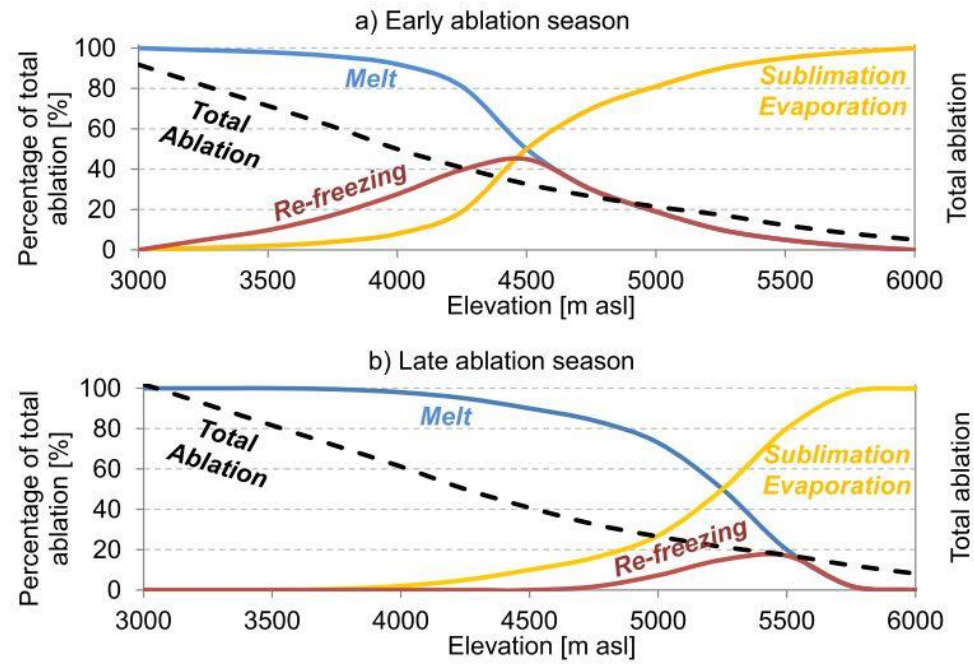


Figure Apx 18: Hypothesized elevation profiles of the dominant components of surface ablation on debris-free glaciers of the semiarid Andes of North-Central Chile during the (a) early and (b) late ablation season. Extracted from Ayala et al., 2017.